

Robust support vector model based on bounded asymmetric elastic net loss for binary classification

Haiyan Du, Hu Yang*

College of Mathematics and Statistics, Chongqing University, Chongqing, 401331, China

Abstract

In this paper, we propose a novel bounded asymmetric elastic net (L_{baen}) loss function and combine it with the support vector machine (SVM), resulting in the BAEN-SVM. The L_{baen} is bounded and asymmetric and can degrade to the asymmetric elastic net hinge loss, pinball loss, and asymmetric least squares loss. BAEN-SVM not only effectively handles noise-contaminated data but also addresses the geometric irrationalities in the traditional SVM. By proving the violation tolerance upper bound (VTUB) of BAEN-SVM, we show that the model is geometrically well-defined. Furthermore, we derive that the influence function of BAEN-SVM is bounded, providing a theoretical guarantee of its robustness to noise. The Fisher consistency of the model further ensures its generalization capability. Since the L_{baen} loss is non-convex, we designed a clipping dual coordinate descent-based half-quadratic algorithm to solve the non-convex optimization problem efficiently. Experimental results on artificial and benchmark datasets indicate that the proposed method outperforms classical and advanced SVMs, particularly in noisy environments.

Keywords: Bounded asymmetric elastic net loss, Binary classification, Geometrical rationality, Robustness, Half-quadratic algorithm

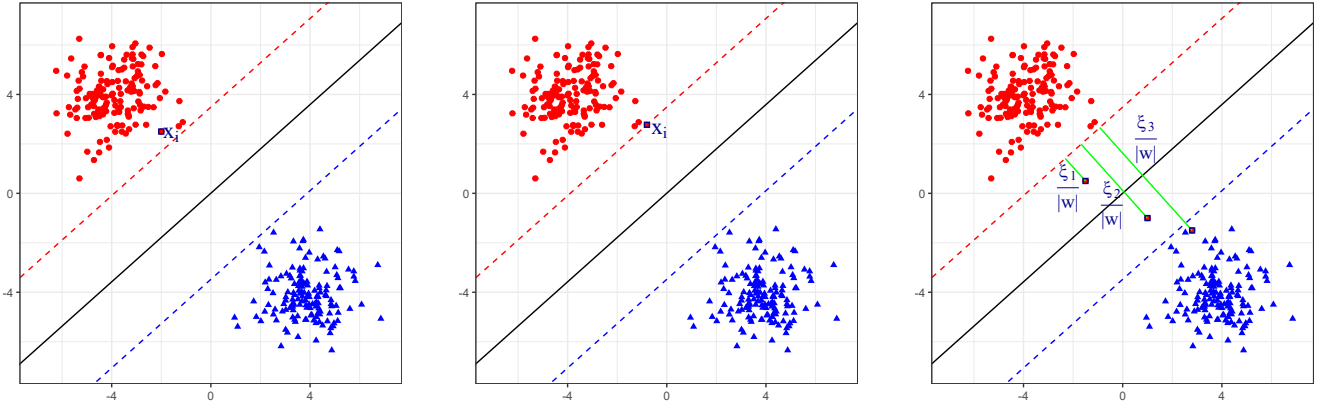
1. Introduction

Support Vector Machine (SVM), first proposed by Vapnik (Vapnik, 2006), aims to construct a binary classification hyperplane by maximizing the margin. Due to their geometric simplicity and solid statistical foundations, SVMs have been widely applied in various fields, including image recognition (Wang, 2025), medical diagnosis (Li et al., 2025), financial forecasting (Kuo and Chiu, 2024), and industrial inspection (Zhang et al., 2025). However, the original hard-margin SVM enforces strict constraints, assuming all samples are linearly separable and outside the margin, which is rarely satisfied in practice. To address this, Cortes and Vapnik (1995) introduced the soft-margin SVM by adding slack variables ξ_i to allow certain violations.

Despite extensive research demonstrating the effectiveness of support vector classifiers, there are still limitations. Qi et al. (2019) pointed out the standard SVM is not rationally defined in geometric terms of the

*Corresponding author. *Email:* yh@cqu.edu.cn

slack variable. Intuitively, the slack variable should directly relate to the distance between a sample and the boundary hyperplane, as illustrated in Fig. 1. However, Qi et al. (2019) pointed out that this relationship is not



(a) x_i is far from the boundary hyperplane (b) x_i lies on the boundary hyperplane (c) x_i crosses the boundary hyperplane

Fig. 1. The relationship between sample x_i and slack variable ξ_i for SVM

adequately captured by the standard SVM (i.e. $c_1 = 0$ and $c_2 > 0$ in (2)). When samples lie across the margin (Fig. 1(c)), the slack variable $\xi_i = 0$ while the Lagrange multiplier $\alpha_i = c_2$, which may lead to overfitting. Considering the connection between slack variables and generalization, Mangasarian and Musicant (2001) proposed the Lagrangian SVM (LSVM) with a ridge penalty. However, the equality constraints in LSVM (i.e. $c_1 > 0$ and $c_2 = 0$ in (2)) imply that samples on the boundary contribute nothing to the final model (i.e. $\xi_i = 0$ and $\alpha_i = 0$), which contradicts SVM’s principle. To improve this, Qi et al. (2019) proposed the Elastic Net SVM (EN-SVM), which integrates l_1 and l_2 penalties on slack variables. Nevertheless, both LSVM and EN-SVM rely on convex loss functions and lack robustness.

The standard SVM is sensitive to feature noise (i.e., noise on sample x_i) and label noise (i.e., noise on label y_i). SVM can be viewed within a regularization framework that combines loss and penalty terms. Huang et al. (2014a) noted that hinge loss-based SVM (Hinge-SVM) lacks robustness to feature noise because the decision hyperplane is significantly disrupted by noise near the boundary. To improve robustness against feature noise, Huang et al. (2014a) proposed Pin-SVM introducing the pinball loss, although this reduced model sparsity. Shen et al. (2017) improved sparsity using a truncated pinball loss (\overline{pin} -SVM), but this introduced non-differentiability at the truncation. Subsequent works proposed smoother and asymmetric alternatives, such as Linex-SVM (Ma et al., 2019), smooth ramp and pinball losses (Wang et al., 2008; Zhu et al., 2020), and semi-smooth pinball variants (Wang et al., 2023). However, SVMs based on improved pinball loss variants still suffer from the same geometric irrationality as the standard SVM.

To address label noise, researchers have proposed several bounded loss functions. Tang et al. (2021a) introduced a bounded Linex loss function (Blinex) into the C-SVM, proposing the CSKB. Fu et al. (2023)

proposed a general framework for bounded loss functions (BLFR) inspired by the Linex loss, and extended this framework into the Robust Loss for Machine Learning (RLM) (Fu et al., 2024) in SVM to obtain FHSVM and FLSSVM. Zhang and Yang (2024) introduced the BQ-SVM and BALS-SVM (Zhang and Yang, 2025) based on the BLFR framework. Other scholars truncated unbounded losses directly, such as truncated hinge loss (Wu and Liu, 2007), generalized ramp loss (Wang and Shao, 2024), valley loss (Tang et al., 2021b), capped asymmetric elastic net loss (Qi and Yang, 2023), and truncated huber loss (Wang and Shao, 2023). However, truncating these loss functions introduces non-differentiable points and increases optimization burden.

To address the above problems, inspired by EN-SVM (Qi et al., 2019) and the RLM framework (Fu et al., 2024), we propose a novel bounded asymmetric elastic-net (L_{baen}) loss and combine it with SVM to obtain BAEN-SVM. BAEN-SVM not only inherits the geometrical rationality of EN-SVM, but also effectively copes with noise-polluted data. The primary contributions are summarized as follows:

- We introduce the bounded asymmetric elastic-net loss to achieve stability against feature noise and robustness to label noise. L_{baen} loss is bounded and asymmetric and can degrade to well-known loss functions, including asymmetric elastic-net loss, pinball loss, and asymmetric least squares loss. Therefore, L_{baen} is a flexible loss function against noise.
- We prove that BAEN-SVM satisfies the violation tolerance upper bound (VTUB), showing that the violation tolerance or slack variable between any two samples is determined exclusively by their relative distance. This result provides a solid theoretical foundation for the geometric rationality of BAEN-SVM.
- We derive the influence function to illustrate the robustness of BAEN-SVM. The bounded nature of the influence function ensures that BAEN-SVM remains robust to noise, thereby theoretically guaranteeing its generalization ability.
- We design a clipping dual coordinate descent based on the half-quadratic (clipDCD-based HQ) algorithm to solve BAEN-SVM, transforming the nonconvex optimization problem into an iterative reweighting process. Extensive experiments validate the effectiveness of the proposed BAEN-SVM.

The rest of the paper is organized as follows: Section 2 reviews recent related studies. In Section 3, we construct BAEN-SVM and solve it using the clipDCD-based HQ algorithm. Next, we provide some theoretical analysis on BAEN-SVM properties in Section 4. In Section 5, the results of artificial and benchmark datasets are utilized to confirm the effectiveness of BAEN-SVM. Finally, Section 6 concludes the paper and discusses future research directions.

2. Related work

In this section, we provide a brief review of related works. Let $T = \{(x_1, y_1), (x_2, y_2)\}, \dots, (x_n, y_n)$ represent the set of training samples, where $x_i \in \mathbb{R}^p$ is the i -th sample and $y_i \in \{-1, +1\}$ is the corresponding label. The samples are organized into a data matrix $X \in \mathbb{R}^{n \times p}$. Unless otherwise specified, all vectors are considered column vectors.

2.1. Elastic net loss for SVM

Qi et al. (2019) put forward elastic net (L_{en}) loss, which imposes the elastic-net penalty to slack variables. By introducing L_{en} loss into SVM, Qi proposed an elastic net loss-based SVM (ENSVM) expressed as

$$\begin{aligned} \min_{w, b} \quad & \frac{1}{2} \|w\|_2^2 + \frac{c_1}{2} \xi^T \xi + c_2 e^T \xi, \\ \text{s.t.} \quad & \begin{cases} e - DXw \leq \xi, \\ \xi \geq \mathbf{0}, \end{cases} \end{aligned} \quad (1)$$

where $D = \text{diag}(y_1, y_2, \dots, y_n)$, $\xi = (\xi_1, \dots, \xi_n)^T$ are the slack variables. By introducing the Lagrange multipliers α_1 and α_2 , according to the Karush–Kuhn–Tucker (KKT) conditions, we have

$$\begin{cases} w = X^T D \alpha, \\ c_1 \xi = \alpha_1 + \alpha_2 - c_2 e. \end{cases} \quad (2)$$

When the sample lies on the boundary hyperplane (i.e. $\xi_i = 0$), the corresponding Lagrange multiplier α_i is non-zero, which means the sample is related to the final classification hyperplane. When the sample crosses the boundary hyperplane, the slack variable $\xi_i > 0$ and $c_1 \xi_i = \alpha_i - c_2$, indicates that the Lagrange multiplier is associated with the degree to which the sample crosses the boundary hyperplane. Qi and Yang (2022) showed through the VTUB of ENNHSVM that the elastic net penalty has unique advantages for slack variables. Thus, improving the performance of EN loss is very important.

To improve the ability of EN-SVM to handle feature noise, Qi designed the asymmetric elastic net (L_{aen}) loss (Qi and Yang, 2023) motivated by pinball loss as follows:

$$L_{aen}(z; p, \tau) = \begin{cases} \frac{p}{2} z^2 + (1-p)z, & z \geq 0, \\ \tau \left(\frac{p\tau}{2} z^2 - (1-p)z \right), & z < 0, \end{cases} \quad (3)$$

where $\tau \in [0, 1]$ is derived from the pinball loss and $p \in [0, 1]$ governs the trade-off between the l_1 norm and the l_2 norm. According to (3), L_{aen} like L_{hinge} grows to infinity as $z \rightarrow \infty$, making it highly sensitive to outliers (label noise).

2.2. Bounded loss functions for SVM

To mitigate the impact of label noise, bounded loss functions have been widely adopted due to their robustness. [Fu et al. \(2023\)](#) proposed a general framework for bounded loss functions (BLFR), inspired by the Linex loss. The framework is defined as

$$L(x) = \frac{1}{\lambda} \left(1 - \frac{1}{1 + b \cdot h(x)} \right), \forall \lambda, b > 0, \quad (4)$$

where $h(x)$ represents any unbounded loss function except the linear form, $b > 0$ and $\lambda > 0$ are parameters controlling the steepness and upper bound of $L(x)$. The BLFR framework can smoothly and adaptively bound any non-negative function and retain its inherently elegant properties, including symmetry, differentiability, and smoothness.

Within the BLFR framework, [Zhang and Yang \(2024\)](#) proposed the bounded quantile loss L_{bq} to improve the robustness of Pin-SVM against label noise. The L_{bq} loss is constructed by taking $h(x) = L_{pin}(x)$, which is formulated as

$$L_{bq}(z; \eta, \lambda, \tau) = \frac{1}{\lambda} \left(1 - \frac{1}{1 + \eta L_{pin}(z)} \right). \quad (5)$$

Then [Zhang and Yang \(2024\)](#) integrated L_{bq} loss into SVM to obtain BQ-SVM. Its definition is as follows:

$$\min_{w, b} \frac{1}{2} (\|w\|_2^2 + b^2) + \frac{C}{2} \sum_{i=1}^n L_{bq}(1 - y_i(x_i^T w + b)). \quad (6)$$

Despite its robustness, the L_{bq} loss remains non-differentiable at certain points, thereby increasing the complexity of the optimization process. To address this limitation, [Zhang and Yang \(2025\)](#) proposed the bounded least absolute squares loss L_{bals} by setting $h(x) = L_{als}(x)$, which is formulated as:

$$L_{bals}(z; \eta, \lambda, \tau) = \frac{1}{\lambda} \left(1 - \frac{1}{1 + \eta L_{als}(z)} \right). \quad (7)$$

Then [Zhang and Yang \(2025\)](#) combined L_{bals} loss with SVM to obtain BALS-SVM. Its definition is as follows:

$$\min_{w, b} \frac{1}{2} (\|w\|_2^2 + b^2) + \frac{C}{2} \sum_{i=1}^n L_{bals}(1 - y_i(x_i^T w + b)). \quad (8)$$

However, BALS-SVM and BQ-SVM do not modify the constraint conditions on the slack variables in ALS-SVM and Pin-SVM, respectively. As a result, they inherit certain limitations in geometric terms of the slack variable.

3. Bounded Asymmetric Elastic Net Loss-Based SVM

3.1. The BAEN-SVM Model

To address the three limitations of existing SVM models, motivated by the RLM framework and L_{aen} loss, we propose a new bounded asymmetric elastic net (L_{baen}) loss function. The formulation of L_{baen} is given by

$$L_{baen}(z; \lambda, \eta, \tau, p) = \frac{1}{\lambda} \left(1 - \frac{1}{1 + \eta L_{aen}(z; p, \tau)} \right) = \begin{cases} \frac{1}{\lambda} \left(1 - \frac{1}{1 + \eta (\frac{p}{2} z^2 + (1-p)z)} \right), z \geq 0, \\ \frac{1}{\lambda} \left(1 - \frac{1}{1 + \eta (\tau (\frac{p}{2} z^2 - (1-p)z))} \right), z < 0, \end{cases} \quad (9)$$

where $\eta > 0$, $\lambda > 0$, and $p \in (0, 1)$ are tuning parameters. The parameter $\tau \in [0, 1]$ is derived from the pinball loss and can increase the number of support vectors.

We illustrate the L_{baen} loss for different values of λ , η , τ , and p in Fig. 2 (a), (b), (c), and (d). As shown in Fig. 2, the parameter λ controls the maximum value of $L_{baen}(z)$, while η determines the steepness of the loss curve. A larger value of η causes the loss to reach its upper bound more quickly. The parameter τ governs the asymmetry of the loss function, which improves the model's robustness to feature noise. Additionally, p affects the steepness and sharpness of the curve and is closely related to the geometric properties of BAEN-SVM, as detailed in Section 4.1.

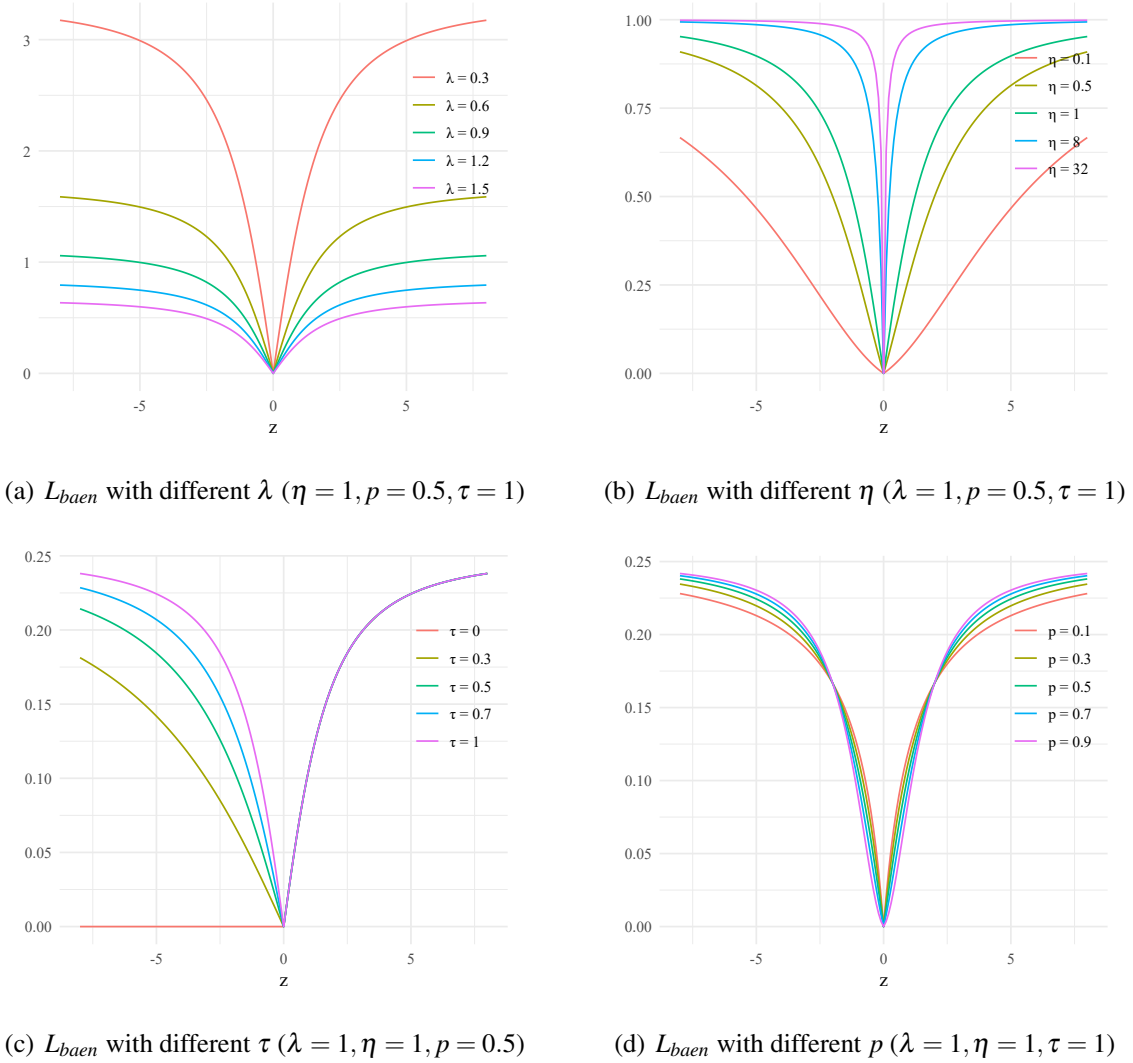


Fig. 2. Different parameter of L_{baen}

In the following, we apply the L_{baen} loss to the traditional SVM to put forward the bounded asymmetric elastic net loss function-based support vector machine (BAEN-SVM) model for the classification problem, which is formulated as

$$\min_{w,b} \frac{1}{2} (\|w\|_2^2 + b^2) + C \sum_{i=1}^n L_{baen}(1 - y_i(w^T x_i + b)), \quad (10)$$

where $C > 0$ is turning parameter, $w \in R^{p \times 1}$ denotes the normal vector of the separating hyperplane, and $b \in R$ represents the intercept. As the intercept b can be included in the normal vector w , we can derive $\tilde{x}_i = (x_i^T, 1)$ and $\tilde{w} = (w^T, b)^T$. Given that λ can be absorbed into C , we set $\lambda = 1$ and define $L_{baen1}(z; \eta, p, \tau) = L_{baen}(z; 1, \eta, p, \tau)$. Then, (10) can be reformulated as

$$\min_w \frac{1}{2} \|\tilde{w}\|_2^2 + C \sum_{i=1}^n L_{baen1}(1 - y_i \tilde{w}^T \tilde{x}_i; \eta, p, \tau). \quad (11)$$

To effectively address nonlinearly separable datasets, we can employ the kernel trick to map each data point into a higher-dimensional space. The feature mapping function $\phi(x)$ is typically defined by a kernel function that satisfies the Mercer theory (Vapnik, 1999). The \tilde{x}_i in problem (11) can be substituted with $\phi(\tilde{x}_i)$ to formulate the dual BAEN-SVM for nonlinearly separable datasets as follows

$$\min_w \frac{1}{2} \|\tilde{w}\|_2^2 + C \sum_{i=1}^n L_{baen1}(1 - y_i \tilde{w}^T \phi(\tilde{x}_i); \eta, p, \tau). \quad (12)$$

3.2. The clipDCD-based HQ Algorithm for BAEN-SVM

The non-convexity of the L_{baen} loss leads to difficulties in the optimization process. To address this, we refer to the work in Zhang and Yang (2025) to solve the model by using the clipping dual coordinate descent-based half-quadratic (Xu et al., 2018) (clipDCD-based HQ) algorithm. By simplifying the calculations, the original optimization problem (12) can be equivalently expressed as

$$\max_{\tilde{w}} -\frac{1}{2} \|\tilde{w}\|_2^2 + C \sum_{i=1}^n \frac{1}{1 + \eta L_{aen}(1 - y_i \tilde{w}^T \phi(\tilde{x}_i))}. \quad (13)$$

We define a convex function $g(\delta) = -2\sqrt{-\delta} - \delta$, where $\delta < 0$. According to conjugate function theory (Boyd, 2004), its conjugate function $g^*(u)$ is given by

$$g^*(u) = \sup_{\delta < 0} \{u\delta - g(\delta)\}. \quad (14)$$

Given that $u\delta - g(\delta) = u\delta + 2\sqrt{-\delta} + \delta$ is a concave function concerning δ . Consequently, by computing the partial derivative of $u\delta - g(\delta)$ concerning δ and equating it to 0, the following relationship is obtained

$$u - \frac{1}{\sqrt{-\delta}} + 1 = 0. \quad (15)$$

The analytical solution of (15) is presented as follows

$$\delta = -\frac{1}{(1+u)^2} < 0. \quad (16)$$

Thus, we have that $(u\delta + 2\sqrt{-\delta} + \delta)|_{\delta = -\frac{1}{(1+u)^2}} = \frac{1}{1+u}$. Consequently, we obtain that

$$g^*(u) = \sup_{\delta < 0} \{u\delta - g(\delta)\} = \frac{1}{1+u}. \quad (17)$$

If we define $u = \eta L_{aen}(z)$ in (17), we get

$$\sup_{v < 0} \{ \eta L_{aen}(z)v - g(\delta) \} = \frac{1}{1 + \eta L_{aen}(z)}, \quad (18)$$

where the supremum is achieved at $\delta = -\frac{1}{(1 + \eta L_{aen}(z))^2} < 0$. Using (18), the objective function in (13) can be equivalently rewritten as

$$\begin{aligned} & -\frac{1}{2} \|\tilde{w}\|_2^2 + C \sum_{i=1}^n \sup_{\delta_i < 0} \{ \eta L_{aen}(1 - y_i \tilde{w}^T \phi(\tilde{x}_i)) \delta_i - g(\delta_i) \} \\ & = \sup_{\delta < 0} \left\{ -\frac{1}{2} \|\tilde{w}\|_2^2 + C \sum_{i=1}^n (\eta L_{aen}(1 - y_i \tilde{w}^T \phi(\tilde{x}_i)) \delta_i - g(\delta_i)) \right\}, \end{aligned} \quad (19)$$

where $\delta = (\delta_1, \delta_2, \dots, \delta_n)^T$. Using (19), we can derive that (13) is equivalent to

$$\max_{\tilde{w}, \delta < 0} -\frac{1}{2} \|\tilde{w}\|_2^2 + C \sum_{i=1}^n (\eta L_{aen}(1 - y_i \tilde{w}^T \phi(\tilde{x}_i)) \delta_i - g(\delta_i)). \quad (20)$$

Next, we design an iterative alternating optimization algorithm to solve (20). In summary, given \tilde{w} , we optimize δ ; given δ , we optimize \tilde{w} . First, assume that we are given \tilde{w}^s at the s -th iteration. Then, (20) can be equivalently rewritten as

$$\max_{\delta^s < 0} \sum_{i=1}^n (\eta L_{aen}(1 - y_i \tilde{w}^s{}^T \phi(\tilde{x}_i)) \delta_i^s - g(\delta_i^s)). \quad (21)$$

Using (17), we can update

$$\delta_i^s = -\frac{1}{(1 + \eta L_{aen}(1 - y_i \tilde{w}^s{}^T \phi(\tilde{x}_i)))^2} < 0. \quad (22)$$

Second, fixing δ to δ^s , we can update \tilde{w}^s by solving the following problem

$$\tilde{w}^s = \arg \min_{\tilde{w}} \frac{1}{2} \|\tilde{w}\|_2^2 + C \sum_{i=1}^n \eta L_{baen}(1 - y_i \tilde{w}^T \phi(\tilde{x}_i)) (-v_i). \quad (23)$$

Let $\omega_i = C\eta(-\delta_i)$, the optimization problem in (23) can be reformulated as a weighted asymmetric elastic net loss support vector machine (AEN-WSVM):

$$\min_{\tilde{w}} \frac{1}{2} \|\tilde{w}\|_2^2 + \sum_{i=1}^n \omega_i L_{aen}(1 - y_i \tilde{w}^T \phi(\tilde{x}_i)). \quad (24)$$

Denoting $\Omega = \text{diag}(\omega_1, \omega_2, \dots, \omega_n)$, then (24) can be rewritten as

$$\begin{aligned} & \min_{\tilde{w}, \xi} \frac{1}{2} \|\tilde{w}\|^2 + \frac{p}{2} \xi^T \Omega \xi + (1-p)e^T \Omega \xi \\ & \text{s.t.} \begin{cases} e - DA\tilde{w} \leq \xi, \\ DA\tilde{w} - e \leq \frac{\xi}{\tau}, \end{cases} \end{aligned} \quad (25)$$

where $A = (\phi(\tilde{x}_1)^T, \phi(\tilde{x}_2)^T, \dots, \phi(\tilde{x}_n)^T)$, $D = \text{diag}(y_1, \dots, y_n) \in \mathbb{R}^{n \times n}$, $e \in \mathbb{R}^{n \times 1}$ is filled with all elements equal to 1, and $\xi = (\xi_1, \dots, \xi_n)^T \in \mathbb{R}^n$ is slack variable. Using Lagrange multipliers $\alpha > 0$ and $\beta > 0$, we can obtain the Lagrange function as below

$$L(\tilde{w}, \xi, \alpha, \beta) = \frac{1}{2} \|\tilde{w}\|^2 + (1-p)e^T \Omega \xi + \frac{p}{2} \xi^T \Omega \xi + \alpha^T (e - DA\tilde{w} - \xi) + \beta^T (DA\tilde{w} - e - \frac{\xi}{\tau}). \quad (26)$$

By computing the partial derivatives with regard to \tilde{w} and ξ and equating the results to 0, we obtain

$$\begin{cases} \tilde{w} = A^T D(\alpha - \beta), \\ p\Omega\xi = \alpha + \frac{\beta}{\tau} - (1-p)\Omega e. \end{cases} \quad (27)$$

In fact, there is a correspondence between α and β . When $\alpha > 0$, we have $e - DA\tilde{w} = \xi$ and $DA\tilde{w} - e - \frac{\xi}{\tau} < 0$, then $\beta \neq 0$. When $\beta > 0$, we have $DA\tilde{w} - e = \frac{\xi}{\tau}$ and $e - DA\tilde{w} - \xi < 0$, then $\alpha \neq 0$. Substituting (27) into the Lagrange function (25), we have

$$\begin{aligned} L(\tilde{w}, \xi, \alpha, \beta) = & -\frac{1}{2}(\alpha - \beta)^T DAA^T D(\alpha - \beta) - \frac{1}{2p}(\alpha + \frac{\beta}{\tau})^T \Omega^{-1}(\alpha + \frac{\beta}{\tau}) \\ & + \frac{1-p}{p}(\alpha + \frac{\beta}{\tau})\Omega e + e^T(\alpha - \beta). \end{aligned} \quad (28)$$

(24) can be transformed into the following equivalent dual problem

$$\begin{aligned} & \min_{\alpha, \beta} \frac{1}{2}(\alpha - \beta)^T DAA^T D(\alpha - \beta) \\ & + \frac{1}{2p}(\alpha + \frac{\beta}{\tau})^T \Omega^{-1}(\alpha + \frac{\beta}{\tau}) - \frac{1-p}{p}e^T(\alpha + \frac{\beta}{\tau}) - e^T(\alpha - \beta) \\ & \text{s.t. } \alpha, \beta \geq 0. \end{aligned} \quad (29)$$

Letting

$$u = \begin{pmatrix} \alpha \\ \beta \end{pmatrix}, Q = \begin{pmatrix} DAA^T D & -DAA^T D \\ -DAA^T D & DAA^T D \end{pmatrix}, S = \frac{1}{\Omega} \begin{pmatrix} I_n & \frac{1}{\tau}I_n \\ \frac{1}{\tau}I_n & \frac{1}{\tau^2}I_n \end{pmatrix}, q = \begin{pmatrix} e + \frac{(1-p)e}{p} \\ -e + \frac{(1-p)e}{p\tau} \end{pmatrix}. \quad (30)$$

Let $H = Q + \frac{S}{p}$, the dual problem of the BAEN-SVM (29) becomes a standard quadratic program

$$\begin{aligned} & \min_u \frac{1}{2}u^T H u - q^T u \\ & \text{s.t. } 0 \leq u. \end{aligned} \quad (31)$$

Finally, we utilize the clipping dual coordinate descent (clipDCD) (Peng et al., 2014) algorithm to solve (31).

The overall solution framework for BAEN-SVM is summarized in Algorithm 1.

After acquiring α^* and β^* from Algorithm 1, we can obtain the final decision function of BAEN-SVM, which is formulated as below

$$f(x) = \sum_{i=1}^n y_i k(\tilde{x}, \tilde{x}_i)(\alpha_i^* - \beta_i^*). \quad (32)$$

3.3. Relationships with other models

The proposed BAEN-SVM is closely related to several widely used support vector machine models. By simplifying the L_{baen} loss function in (9), we obtain

$$L_{baen}(z) = \frac{1}{\lambda} \left(1 - \frac{1}{1 + \eta L_{aen}(z; p, \tau)} \right) = \frac{1}{\lambda} \cdot \frac{\eta L_{aen}(z; p, \tau)}{1 + \eta L_{aen}(z; p, \tau)}. \quad (33)$$

Algorithm 1 clipDCD-based HQ Solver for BAEN-SVM

Input: Training set $D = \{x_i, y_i\}, i = 1, 2, \dots, n$; Maximum number of iterations $h_{\max} \in \mathbb{Z}^+$; Tolerance $\varepsilon \in \mathbb{R}^+$

Output: The optimal solution of (11)

- 1: Set initialize $\delta^0, \alpha^0, \beta^0, u^0, s = 0$.
 - 2: **while** $s \leq h_{\max}$ **do**
 - 3: Compute $\Omega = \text{diag}(-C\eta\delta^s)$.
 - 4: Solving the optimization problem (31) with the clipDCD algorithm to obtain $u^{s+1} = ((\alpha^{s+1})^T, (\beta^{s+1})^T)^T$.
 - 5: **if** $\|u^{s+1} - u^s\|_2 < \varepsilon$ or $s > h_{\max}$ **then**
 - 6: Break.
 - 7: **end if**
 - 8: Update δ^s by (22).
 - 9: let $s = s + 1$
 - 10: **end while**
 - 11: **return** $\alpha^* = \alpha^s, \beta^* = \beta^s$.
-

Letting $\eta = \lambda$ and $\lambda \rightarrow 0$, we have

$$\lim_{\lambda \rightarrow 0} \frac{1}{\lambda} \cdot \frac{\lambda L_{aen}(z; p, \tau)}{1 + \lambda L_{aen}(z; p, \tau)} = L_{aen}(z; p, \tau). \quad (34)$$

This result shows that the L_{baen} loss can degrade into the L_{aen} as $\lambda \rightarrow 0$, implying that BAEN-SVM reduces to the AEN-SVM in this case. It is important to note that the L_{aen} loss can be viewed as a combination of L_{en} loss, L_{pin} loss, and the asymmetric least squares (L_{als}) loss function (Huang et al., 2014a). Specifically, L_{aen} reduce to L_{en} when $\tau = 0$, becomes equivalent to L_{pin} when $p = 0$, and simplifies to the L_{als} for $p = 1$ and $\tau = 1$. Consequently, the BAEN-SVM provides a more general framework encompassing these traditional SVMs as special cases.

Compared with the convex loss functions such as L_{aen} , L_{en} , L_{pin} , and L_{als} , we proposed non-convex L_{baen} loss is less sensitive to label noise due to its boundedness. Specifically, since $\eta > 0$ and $L_{aen}(z)$ increases monotonically with z , we have

$$\lim_{z \rightarrow \infty} L_{baen}(z) = \lim_{z \rightarrow \infty} \frac{1}{\lambda} \cdot \frac{\eta L_{aen}(z)}{1 + \eta L_{aen}(z)} = \lim_{L_{aen}(z) \rightarrow \infty} \frac{1}{\lambda \left(\frac{1}{\eta L_{aen}(z)} + 1 \right)} = \frac{1}{\lambda} \quad (35)$$

This shows that the L_{baen} function is bounded above by $1/\lambda$. As can be seen from the Fig. 3, the proposed L_{baen} loss is not only bounded but also asymmetric under different parameter settings. Therefore, BAEN-SVM exhibits greater robustness to noise. Detailed theoretical proofs are provided in Section 4.3.

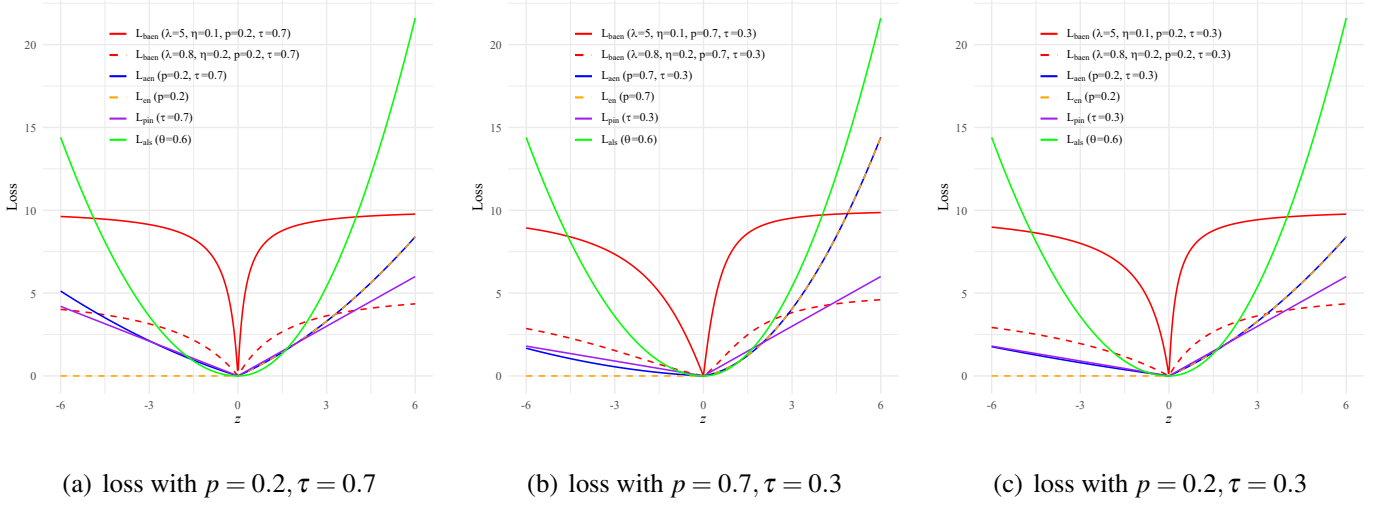


Fig. 3. Loss functions with different parameters

4. Properties of BAEN-SVM

This section analyzes the main properties of our proposed BAEN-SVM, encompassing geometrical rationality, Fisher consistency, noise insensitivity, and computational complexity.

4.1. Geometrical Rationality

In this section, according to [Qi and Yang \(2022\)](#)'s work about violation tolerance upper bound (VTUB), we discuss the geometric properties of BAEN-SVM. In SVM, the slack variable is interpreted as the violation tolerance concerning the optimal hyperplane, which is closely linked to the model's generalization performance. [Qi and Yang \(2022\)](#) derived the VTUB to describe the connection between the slack variables and the distance of any two samples violating the constraints. Next, we state the result with the following two theorems:

Theorem 1. *Given n samples and parameter $p \in (0, 1)$, if the training samples x_i and x_j belong to the same class and both violate the constraints of BAEN-SVM, for ξ_i and ξ_j are estimated by BAEN-SVM, we have*

$$|\xi_i - \xi_j| \leq p(\vartheta_1 + p\vartheta_n)\sqrt{n}\|\tilde{X}\|_F \cdot d_{ij}, \quad (36)$$

where $\tilde{X} = (X, e)$, $\|\tilde{X}\|_F$ is the Frobenius norm of \tilde{X} , ϑ_1 and ϑ_n are the smallest and the largest eigenvalues of $\tilde{X}^T \tilde{X}$, d_{ij} is the Euclidean distance between x_i and x_j .

Proof. The Lagrangian function for the dual problem (31) can be written as

$$L = \frac{1}{2}u^T H u - q^T u - \sum_{i=1}^{2n} k_j u_j, \quad (37)$$

where k_j are the nonnegative Lagrangian multipliers, $j = 1, \dots, 2n$. Let $k = (k_1, \dots, k_{2n})^T$, then the corresponding KKT condition can be written as

$$\begin{cases} \frac{\partial L}{\partial u} = Hu - q - k = 0, \\ k_j u_j = 0. \end{cases} \quad (38)$$

Now we pay attention to the strictly positive portion of u , represented by u_R , where $R = \{j | u_j > 0, j = 1, \dots, 2n\}$ is the related index set that satisfies $|R| = d$. The partial derivation of (37) with respect to u_R be given as

$$\frac{\partial L}{\partial u_R} = (Q_{RR} + \frac{S_{RR}}{p})u_R + u_{R+n} - q_R - k_R = 0, \quad (39)$$

where $(\cdot)_R$ denotes a sub-vector including elements from vector (\cdot) that corresponds to R and $(\cdot)_{RR}$ is a sub-matrix formed by the rows and columns of matrix (\cdot) corresponding to R . Where $R+n$ denotes the index set formed by adding n to each element of R . Since $\alpha_j = 0$ as $\beta_j \neq 0$ and $\beta_j = 0$ as $\alpha_j \neq 0$, then we have $u_{R+n} = 0$ when $u_R > 0$. According to the second equation in (38) and $u_R > 0$, then we can get $k_R = 0$ and

$$u_R = (Q_{RR} + \frac{S_{RR}}{p})^{-1} q_R. \quad (40)$$

Based on the expression of Q and S in (30), we can deduce that $S_{RR} = I_{RR}$, $q_R = \frac{1}{p} e_R$ and $Q_{RR} = \tilde{X}_R [(\tilde{X}^T \tilde{X})^{-1}] \tilde{X}_R^T$. Let $(\tilde{X}^T \tilde{X})^{-1} = M$, we obtain that

$$u_R = (\tilde{X}_R M \tilde{X}_R^T + \frac{I_{RR}}{p})^{-1} (\frac{1}{p} e_R). \quad (41)$$

Then, by the Woodbury Theorem (Bhatia, 2013) in (40), we have

$$u_R = (pI_{RR} - p^2 \tilde{X}_R G \tilde{X}_R^T) (\frac{1}{p} e_R - u_{R+n}), \quad (42)$$

where $G = (M^{-1} + p \tilde{X}_R^T \tilde{X}_R)^{-1}$. Hence, for any u_i and u_j in u_R , we obtain

$$|u_i - u_j| = p^2 \left| (\tilde{x}_i - \tilde{x}_j)^T G \tilde{X}_R^T (\frac{1}{p} e_R) \right|, \quad (43)$$

where \tilde{x}_j respects the j -th row of \tilde{X} .

Since G is a Hermitian matrix, we can apply the Cauchy-Schwarz inequality to derive that

$$\begin{aligned} & \left| (\tilde{x}_i - \tilde{x}_j)^T G \tilde{X}_R^T (\frac{1}{p} e_R) \right|^2 \\ & \leq (\tilde{x}_i - \tilde{x}_j)^T G (\tilde{x}_i - \tilde{x}_j) \cdot \left(\frac{1}{p} e_R \right)^T \tilde{X}_R G \tilde{X}_R^T \left(\frac{1}{p} e_R \right). \end{aligned} \quad (44)$$

For $(\tilde{x}_i - \tilde{x}_j)^T G (\tilde{x}_i - \tilde{x}_j)$, by the Rayleigh-Ritz Theorem (Bhatia, 2013), we have

$$(\tilde{x}_i - \tilde{x}_j)^T G (\tilde{x}_i - \tilde{x}_j) \leq \gamma_{\max}(G) \cdot \|\tilde{x}_i - \tilde{x}_j\|^2. \quad (45)$$

Since $\tilde{x}_i = (x_i^T, 1)^T$, then $\|\tilde{x}_i - \tilde{x}_j\|^2 = \|x_i x_j\|^2 = d_{ij}^2$. Thus, (45) can be rewritten as

$$(\tilde{x}_i - \tilde{x}_j)^T G (\tilde{x}_i - \tilde{x}_j) \leq \gamma_{\max}(G) \cdot d_{ij}^2, \quad (46)$$

where d_{ij} is the Euclidean distance between x_i and x_j . $\gamma_{\max}(G)$ is the largest eigenvalue of the matrix G .

For $\left(\frac{1}{p}e_R - u_{R+n}\right)^T \tilde{X}_R G \tilde{X}_R^T \left(\frac{1}{p}e_R - u_{R+n}\right)$, similarly, we get

$$\begin{aligned} \left(\frac{1}{p}e_R\right)^T \tilde{X}_R G \tilde{X}_R^T \left(\frac{1}{p}e_R\right) &\leq \gamma_{\max}(G) \left(\frac{1}{p}e_R\right)^T \tilde{X}_R \tilde{X}_R^T \left(\frac{1}{p}e_R\right) \\ &\leq \gamma_{\max}(G) \cdot \left(\frac{1}{p^2}\right) n \|\tilde{X}_R\|_F^2 \\ &\leq \gamma_{\max}(G) \cdot \left(\frac{1}{p^2}\right) n \|\tilde{X}\|_F^2, \end{aligned} \quad (47)$$

where $\|\tilde{X}\|_F = \sqrt{\sum_{i,j} d_{ij}^2}$ is the Frobenius norm of \tilde{X} .

Taking (46) and (47) into (44), we have

$$|u_i - u_j| \leq p \gamma_{\max}(G) \sqrt{n} \|\tilde{X}\|_F \cdot d_{ij}. \quad (48)$$

Since $\tilde{X}^T \tilde{X}$ and $\tilde{X}_R^T \tilde{X}_R$ both are Hermite matrices, then by the Weyl Theorem, it holds for

$$\begin{aligned} \gamma_{\max}(G) &= \gamma_{\min}((\tilde{X}^T \tilde{X})^{-1})^{-1} + p \tilde{X}_R^T \tilde{X}_R \\ &\leq \gamma_{\min}((\tilde{X}^T \tilde{X})^{-1})^{-1} + \gamma_{\max}(p \tilde{X}_R^T \tilde{X}_R) \\ &\leq \gamma_{\max}((\tilde{X}^T \tilde{X})^{-1}) + \gamma_{\max}(p \tilde{X}_R^T \tilde{X}_R) \\ &\leq \gamma_{\min}(\tilde{X}^T \tilde{X}) + p \gamma_{\max}(\tilde{X}_R^T \tilde{X}_R), \end{aligned} \quad (49)$$

where $\gamma_{\min}(\tilde{X}^T \tilde{X})$ is the smallest eigenvalues of $\tilde{X}^T \tilde{X}$. According to Sturm Theorem (Bhatia, 2013), we have $\gamma_{\max}(\tilde{X}_R^T \tilde{X}_R) \leq \gamma_{\max}(\tilde{X}^T \tilde{X})$. Let $\vartheta_1 = \gamma_{\min}(\tilde{X}^T \tilde{X})$ and $\vartheta_n = \gamma_{\max}(\tilde{X}^T \tilde{X})$, combining (48) and (49), we conclude that

$$|u_i - u_j| \leq p(\vartheta_1 + p\vartheta_n) \sqrt{n} \|\tilde{X}\|_F \cdot d_{ij}. \quad (50)$$

Finally, according to the KKT condition (27) for ξ , if $\xi_i > 0$, we have

$$\begin{cases} p\Omega\xi_i + (1-p)\omega_i = \alpha_i = u_i, & i = 1, \dots, n, \\ \tau(p\Omega\xi_i + (1-p)\omega_i) = \beta_i = u_i, & i = n+1, \dots, 2n. \end{cases} \quad (51)$$

Then we have

$$|\xi_i - \xi_j| \leq p(\vartheta_1 + p\vartheta_n) \sqrt{n} \|\tilde{X}\|_F \cdot d_{ij}. \quad (52)$$

The proof is completed. \square

Remark 1. According to Theorem 1, the violation tolerances of samples x_i and x_j for a given dataset and parameter $p \in (0, 1)$ depend only on the distance between them, i.e., the closer the samples are to each other, the closer the corresponding VTUB are. The result aligns with the geometric perspective of SVM.

Remark 2. The formula (51) shows that $u_i \neq 0$ when $\xi_i = 0$, indicating that the sample points lying on the boundary hyperplane in BAEN-SVM still impact the position of the decision hyperplane. It compensates for the geometric irrationality that exists in LSVM and BALS-SVM.

Remark 3. It is important to note that BAEN-SVM can degenerate into BQ-SVM when p equals zero. However, equation (52) does not hold for $p = 0$, which implies that BQ-SVM do not satisfy geometric rationality.

Similarly, we can obtain the VTUB of BAEN-SVM in the nonlinear case.

Theorem 2. Given n samples, parameter $p \in (0, 1)$ and kernel K , if training samples x_i and x_j belong to the same class, which both violate the constraints of BAEN-SVM, for ξ_i and ξ_j are estimated by BAEN-SVM, we have

$$|\xi_i - \xi_j| \leq p(\vartheta_1^K + p\vartheta_n^K)\sqrt{n}\|\tilde{X}_K\|_F \cdot d_{ij}^K. \quad (53)$$

where $\tilde{X}_K = (K(X, X^T), e)$, $\|\tilde{X}_K\|_F$ is the Frobenius norm of \tilde{X}_K , ϑ_1^K and ϑ_n^K are the smallest and the largest eigenvalues of $\tilde{X}_K^T \tilde{X}_K$, d_{ij}^K is the Euclidean distance between x_i^K and x_j^K .

The proof follows similarly to the linear case, with the only difference being the replacement of \tilde{X} with \tilde{X}_K . So, the proof processing is omitted.

4.2. Fisher Consistency

A fundamental property of a binary classifier $f : X \rightarrow Y$ is whether it is Fisher consistent, which guarantees that optimizing a surrogate loss does not prevent searching for a discriminant function that achieves the Bayes' optimal risk. Assuming the training samples $\{(x_i^T, y_i)\}_{i=1}^n$ are independently derived from $\rho(X, Y)$, where $Y \in \{-1, +1\}$. Let $p(x) = \text{Prob}(y = -1|X = x)$ represent the conditional probability of the negative class given $X = x$. The Bayes classifier is expressed as follows:

$$f_C(x) = \begin{cases} -1, \text{Prob}(y = +1|x) < \text{Prob}(y = -1|x), \\ +1, \text{Prob}(y = +1|x) > \text{Prob}(y = -1|x). \end{cases} \quad (54)$$

For any loss function $L(\cdot)$, we define the expected risk of a classifier $f : X \rightarrow Y$ as

$$R_{L,\rho}(f) = \int_{X \times Y} L(1 - yf(x))d\rho. \quad (55)$$

By minimizing the expected risk $R_{L,\rho}(f)$ over all measurable functions, the function $f_{L,\rho}(x)$ is defined as

$$f_{L,\rho}(x) = \arg \min_v \int_Y L(1 - yv)d\rho(y|x), \forall x \in X, \quad (56)$$

where $\rho(y|x)$ is the conditional distribution of y at given x .

Zhang and Yang (2025) states a theorem that can be used to easily check if a loss function under BLFR is Fisher consistent. Next, we prove that our proposed L_{baen} loss satisfies Fisher consistency. We first introduce the following lemma by Zhang and Yang (2025):

Lemma 1. *If a function h satisfies the following two assumptions:*

1. $h(1+v) > h(1-v), \forall v > 0$.
2. $h'(1) \neq 0$ exists.

then the function $f_{L_{BLFR},\rho}$ which minimizes the L_{BLFR} -loss's expected risk over all measurable functions $f : X \rightarrow Y$ has the same sign as Bayes classifier, i.e., $\text{sign}(f_{L_{BLFR},\rho}(x)) = f_C(x), \forall x \in X$.

The proof can be found in Zhang and Yang (2025).

Theorem 3. *The L_{baen} loss function is Fisher consistent, and $f_{L_{baen},\rho}$ by minimizing the L_{baen} -loss's expected risk over all measurable functions $f : X \rightarrow Y$ has the same sign as Bayes classifier, i.e., $\text{sign}(f_{L_{baen},\rho}(x)) = f_C(x), \forall x \in X$.*

Proof. Let

$$h(z) = L_{aen}(z) = \begin{cases} \frac{p}{2}z^2 + (1-p)z, & z \geq 0, \\ \tau(\frac{p\tau}{2}z^2 - (1-p)z), & z < 0, \end{cases} \quad (57)$$

where $p \in (0, 1)$ and $\tau \in [0, 1]$. By the definition of $h(z)$, if $0 < z \leq 1$, we have $h(1+z) > h(1-z)$. If $z \geq 1$, we have $h(1+z) - h(1-z) = \frac{p}{2}(1-\tau^2)(z^2+1) + p(1+\tau^2)z + 2(1-p)$. Since $p \in (0, 1)$ and $\tau \in [0, 1]$, then $h(1+z) - h(1-z) > 0$. Hence, it $L_{aen}(z)$ satisfies the first condition.

Since

$$h(z) = \begin{cases} pz + 1 - p, & z \geq 0, \\ \tau(p\tau z - 1 + p), & z < 0, \end{cases} \quad (58)$$

then $h'(1) = 1$, thus $h'(1) \neq 0$ exists. Using the above results and lemmas, we infer that the function $f_{L_{baen},\rho}$ by minimizing the L_{baen} -loss's expected risk over all measurable functions $f : X \rightarrow Y$ has the same sign as Bayes classifier, i.e., $\text{sign}(f_{L_{baen},\rho}(x)) = f_C(x), \forall x \in X$. \square

4.3. Noise Insensitivity

4.3.1. Robust to Label Noise

Hampel (1974) introduced the influence function, which is designed to measure the stability of the estimators against infinitesimal contamination. For a robust estimator, the influence function should be bounded (Hampel, 1974; Wang et al., 2013). we now analyze the influence function of BAEN-SVM.

Let $(x_0^T, y_0)^T$ denote a sample point with mass probability distribution p_0 . Consider the distribution \mathcal{F} of $(x^T, y)^T \in \mathbb{R}^{p+1}$. We defined $\mathcal{F}_\theta = (1-\theta)\mathcal{F} + \theta p_0$ to represent the mixed distribution of \mathcal{F} and p_0 ,

where $\theta \in (0, 1)$ is the proportion parameter. The optimal solutions under the distribution \mathcal{F} and the mixed distribution \mathcal{F}_θ are denoted as w_0^* and w_θ^* , respectively.

$$\begin{cases} w_0^* = \arg \min_w [nC \int L_{baen}(z) d\mathcal{F} + \frac{1}{2} \|w\|_2^2], \\ w_\theta^* = \arg \min_w [nC \int L_{baen}(z) d\mathcal{F}_\theta + \frac{1}{2} \|w\|_2^2]. \end{cases} \quad (59)$$

The influence function at $(x_0^T, y_0)^T$ can be expressed as

$$\text{IF}(x_0, y_0; w_0^*) = \lim_{\theta \rightarrow 0^+} \frac{w_\theta^* - w_0^*}{\theta}, \quad (60)$$

provided that the limit exists. Before presenting the result, we make the following common assumptions about the distribution of the training dataset.

Assumption 1. *The random variable $x \in X$ has a finite second moment.*

Assumption 2. $W_0 = (\frac{1}{nC}I + \int xx^T \nabla^2 L_{baen}(z(x, y, w_0^*)) d\mathcal{F})$ is invertible.

[Assumption 1](#) is common in statistics, and it is easy to satisfy that the dimension of the sample is finite. If W_0 is not invertible, then there exists an eigenvalue of $\int xx^T \nabla^2 L_{baen}(z(x, y, w_0^*)) d\mathcal{F}$ exactly equal to $\frac{1}{nC}$, which is a small probability event. Therefore, both [Assumption 1](#) and [Assumption 2](#) are exceedingly weak.

Theorem 4. *For linear BAEN-SVM with η , τ , p and λ fixed, the influence function $\text{IF}(x_0, y_0; w_0^*)$ can be calculated using this formula*

$$\text{IF}(x_0, y_0; w_0^*) = W_0^{-1} \left(-\frac{1}{nC} w_0 - \gamma_0 - \nabla L_{baen}(z(x_0, y_0, w_0^*)) \frac{\partial z(x_0, y_0, w_0^*)}{\partial w_0^*} \right) \quad (61)$$

where $W_0 = (\frac{1}{nC}I + \int xx^T \frac{\partial z(x, y, w_0^*)}{\partial (w_0^*)^T} \nabla^2 L_{baen}(z(x, y, w_0^*)) d\mathcal{F})$, and

$$\nabla^2 L_{baen}(z) = \begin{cases} \frac{1}{\lambda} \cdot \frac{\eta \tau^2 p (1 + \eta \tau (\frac{p\tau}{2} z^2 - (1-p)z)) - 2\eta^2 \tau^2 (p\tau z - (1-p))^2}{[1 + \eta \tau (\frac{p\tau}{2} z^2 - (1-p)z)]^3}, & z < 0, \\ [\frac{\eta \tau^2 p - 2\eta^2 \tau^2 (1-p)^2}{\lambda}, \frac{\eta p - 2\eta^2 (1-p)^2}{\lambda}], & z = 0, \\ \frac{1}{\lambda} \cdot \frac{\eta p (1 + \eta (\frac{p}{2} z^2 + (1-p)z)) - 2\eta^2 (pz + 1 - p)^2}{[1 + \eta (\frac{p}{2} z^2 + (1-p)z)]^3}, & z > 0, \end{cases} \quad (62)$$

where $z = 1 - yx^T w_\theta^*$ and

$$\gamma_0 = \int \frac{\partial}{\partial \theta} (\zeta_0 \cdot \frac{\partial z(x, y, w_\theta^*)}{\partial w_\theta^*}) d\mathcal{F} |_{\theta=0}, \quad (63)$$

where $\zeta_0(\theta, x, y) \in [-\frac{\eta \tau (1-p)}{\lambda}, \frac{\eta (1-p)}{\lambda}]$, and $\text{IF}(x_0, y_0; w_0^*)$ is bounded.

Proof. By the KKT conditions, w_θ^* must satisfies

$$w_\theta^* = -nC \int \nabla L_{baen}(z(x, y, w_\theta^*)) \frac{\partial z(x, y, w_\theta^*)}{\partial w_\theta^*} d\mathcal{F}_\theta, \quad (64)$$

Since $\mathcal{F}_\theta = (1 - \theta)\mathcal{F} + \theta p_0$, (64) can be expressed as

$$-\frac{1}{nC}w_\theta^* = (1 - \theta) \int \nabla L_{baen}(z(x, y, w_\theta^*)) \frac{\partial z(x, y, w_\theta^*)}{\partial w_\theta^*} d\mathcal{F} + \theta \nabla L_{baen}(z(x_0, y_0, w_\theta^*)) \frac{\partial z(x_0, y_0, w_\theta^*)}{\partial w_\theta^*}. \quad (65)$$

By differentiating with regard to θ in both sides of (65) and letting $\theta \rightarrow 0$, we obtain

$$\begin{aligned} \left. \frac{1}{nC} \frac{\partial w_\theta^*}{\partial \theta} \right|_{\theta=0} &= \int \nabla L_{baen}(z(x, y, w_\theta^*)) \frac{\partial z(x, y, w_\theta^*)}{\partial w_\theta^*} d\mathcal{F} \Big|_{\theta=0} \\ &\quad - \int \nabla^2 L_{baen}(z(x, y, w_\theta^*)) \frac{\partial z(x, y, w_\theta^*)}{\partial w_\theta^*} \frac{\partial z(x, y, w_\theta^*)}{\partial (w_\theta^*)^T} d\mathcal{F} \frac{\partial w_\theta^*}{\partial \theta} \Big|_{\theta=0} \\ &\quad - \nabla L_{baen}(z(x_0, y_0, w_\theta^*)) \frac{\partial z(x_0, y_0, w_\theta^*)}{\partial w_\theta^*} \Big|_{\theta=0} - \gamma_0, \end{aligned} \quad (66)$$

where

$$\gamma_0 = \int \frac{\partial}{\partial \theta} (\zeta_0 \cdot \frac{\partial z(x, y, w_\theta^*)}{\partial w_\theta^*}) d\mathcal{F} \Big|_{\theta=0}, \quad (67)$$

where $\zeta_0 \in \left[-\frac{\eta\tau(1-p)}{\lambda}, \frac{\eta(1-p)}{\lambda}\right]$ from the first derivative of the L_{baen} loss function (9). Combining (64) and (66), we have

$$\begin{aligned} \left(\frac{1}{nC}I + \int \nabla^2 L_{baen}(z(x, y, w_0^*)) \frac{\partial z(x, y, w_0^*)}{\partial w_0^*} \frac{\partial z(x, y, w_0^*)}{\partial (w_0^*)^T} d\mathcal{F}\right) \text{IF}(x_0, y_0; w_0^*) &= \\ -\frac{1}{nC}w_0 - \nabla L_{baen}(z(x_0, y_0, w_0^*)) \frac{\partial z(x_0, y_0, w_0^*)}{\partial w_0^*} - \gamma_0. \end{aligned} \quad (68)$$

where I is an identity matrix of the proper size. We denote

$$W_0 = \left(\frac{1}{nC}I + \int \frac{\partial z(x, y, w_0^*)}{\partial w_0^*} \frac{\partial z(x, y, w_0^*)}{\partial (w_0^*)^T} \nabla^2 L_{baen}(z(x, y, w_0^*)) d\mathcal{F}\right). \quad (69)$$

According to Assumption 2, the influence function of BAEN-SVM is specified as

$$\text{IF}(x_0, y_0; w_0^*) = W_0^{-1} \left(-\frac{1}{nC}w_0 - \gamma_0 - \nabla L_{baen}(z(x_0, y_0, w_0^*)) \frac{\partial z(x_0, y_0, w_0^*)}{\partial w_0^*}\right). \quad (70)$$

In the following, we prove that $\text{IF}(x_0, y_0; w_0^*)$ is bounded. According to (70), if we want to analyze the boundedness of the influence function, it is necessary to examine the gradient properties of the L_{baen} loss function. Reviewing the L_{baen} loss, the sub-gradient of L_{baen} with respect to z is given by the following formula:

$$\nabla L_{baen}(z) = \begin{cases} \frac{\eta\tau(p\tau z - (1-p))}{\lambda(1 + \eta\tau(\frac{p^2}{2}z^2 - (1-p)z))^2}, & z < 0, \\ \left[-\frac{\eta\tau(1-p)}{\lambda}, \frac{\eta(1-p)}{\lambda}\right], & z = 0, \\ \frac{\eta(pz + 1 - p)}{\lambda(1 + \eta(\frac{p}{2}z^2 + (1-p)z))^2}, & z > 0. \end{cases} \quad (71)$$

By (9) and (71), $\frac{\eta(pz + 1 - p)}{\lambda(1 + \eta(\frac{p}{2}z^2 + (1-p)z))^2} > 0$ when $z \geq 0$, which implies that $L_{baen}(z)$ is monotonically increasing for $z \geq 0$. According to (35), we know that $L_{baen}(z) \rightarrow \frac{1}{\lambda}$ as $z \rightarrow \infty$. Thus, $L_{baen}(z + \varepsilon) - L_{baen}(z) \rightarrow 0$ as z tends to infinity. Since $L_{baen}(z)$ is continuous and differentiable almost everywhere, then we have

$$\nabla L_{baen}(z) = \lim_{\varepsilon \rightarrow 0} \frac{L_{baen}(z + \varepsilon) - L_{baen}(z)}{\varepsilon} \quad (72)$$

exists and satisfies $\nabla L_{baen} \rightarrow 0$ as z tends to infinity. The case of $z < 0$ can be analyzed analogously. Hence, we obtain that $\nabla L_{baen} \rightarrow 0$ as $x \rightarrow \infty$.

According to [Assumption 1](#) and (70), we have

$$\|\mathbf{IF}(x_0, y_0; w_0^*)\| \leq \lambda_{\min}(W_0) \left(\left\| \frac{1}{nC} w_0 \right\| + \|\gamma_0\| + \|\nabla L_{baen}(z(x_0, y_0, w_0^*))\| \left\| \frac{\partial z(x_0, y_0, w_0^*)}{\partial w_0^*} \right\| \right), \quad (73)$$

where $\lambda_{\min}(\cdot)$ is the smallest eigenvalue of a matrix. Since ζ_0 is bounded and continuous for θ over closed intervals, its derivative for θ is also bounded. Consequently, γ_0 is also bounded. Therefore, with the above analysis, we have $\lambda_{\min}(W_0) \left(\left\| \frac{1}{nC} w_0 \right\| + \|\gamma_0\| + \|\nabla L_{baen}(z(x_0, y_0, w_0^*))\| \left\| \frac{\partial z(x_0, y_0, w_0^*)}{\partial w_0^*} \right\| \right) \leq \infty$. Then (73) is bounded, which means that the influence function of BAEN-SVM is bounded. \square

4.3.2. Robust to Feature noise

In the subsection, we employ the methodology of [Huang et al. \(2014a\)](#) to demonstrate the robustness of BAEN-SVM against feature noise.

According to KKT conditions, the optimality condition for BAEN-SVM (11) can be written as

$$0 \in \frac{w}{C} - \frac{1}{2} \sum_{i=1}^n \nabla L_{baen}(1 - y_i x_i^T w; \lambda, \eta, p, \tau) y_i x_i. \quad (74)$$

According to the sub-gradient of L_{baen} (71), for given w , the index set is divided into three sets

$$\begin{aligned} S_+^w &= \{i : 1 - y_i x_i^T w > 0\}, \\ S_-^w &= \{i : 1 - y_i x_i^T w < 0\}, \\ S_0^w &= \{i : 1 - y_i x_i^T w = 0\}. \end{aligned} \quad (75)$$

Due to the presence of $\zeta \in \left[-\frac{\eta\tau(1-p)}{\lambda}, \frac{\eta(1-p)}{\lambda} \right]$, (74) can be equivalently rewritten as

$$\frac{w}{C} - \sum_{i \in S_-^w} \frac{\eta\tau(p\tau z - (1-p))}{\lambda \left(1 + \eta\tau \left(\frac{p\tau}{2} z^2 - (1-p)z\right)\right)^2 y_i x_i} - \sum_{i \in S_+^w} \frac{\eta(pz + 1 - p)}{\lambda \left(1 + \eta \left(\frac{p}{2} z^2 + (1-p)z\right)\right)^2 y_i x_i} - \sum_{i \in S_0^w} \zeta_i y_i x_i = 0. \quad (76)$$

Since S_0^w is determined by equalities, it is reasonable to conclude that the size of S_0^w is much smaller than that of S_+^w and S_-^w . Consequently, the contribution of S_0^w to (76) is relatively weak. Then, we can approximately determine w from S_+^w and S_-^w . Thus, (76) is equal to

$$\frac{w}{C} - \sum_{i \in S_-^w} \frac{\eta\tau(p\tau z - (1-p))}{\lambda \left(1 + \eta\tau \left(\frac{p\tau}{2} z^2 - (1-p)z\right)\right)^2 y_i x_i} - \sum_{i \in S_+^w} \frac{\eta(pz + 1 - p)}{\lambda \left(1 + \eta \left(\frac{p}{2} z^2 + (1-p)z\right)\right)^2 y_i x_i} \cong \mathbf{0}. \quad (77)$$

Since $\lambda > 0, \eta > 0$, then (77) can be written as

$$\frac{w}{C} + \sum_{i \in S_-^w} \tau(1-p - p(1 - y_i x_i^T w)\tau) - \sum_{i \in S_+^w} (p(1 - y_i x_i^T w) + 1 - p)y_i x_i \cong \mathbf{0}. \quad (78)$$

Since $\tau(1 - p - p(1 - y_i x_i^T w) \tau) y_i x_i$ and $(p(1 - y_i x_i^T w) + 1 - p) y_i x_i$ are positive, suggesting that τ plays a key role in balancing the contributions from S_+^w and S_-^w in BAEN-SVM. According to (78), as τ approaches 0, the final separating hyperplane is predominantly influenced by sample points from S_+^w . When τ is close to 1, both S_+^w and S_-^w contain a large number of sample points, indicating that the model is less sensitive to zero-mean feature noise near the decision boundary. Therefore, we can show that BAEN-SVM is robust to feature noise.

4.4. Complexity Analysis

This subsection provides a detailed analysis of the time complexity of the proposed BAEN-SVM method. Our algorithm has a computational advantage over existing algorithms designed for solving non-convex models, primarily owing to its efficient strategy for addressing the associated quadratic optimization subproblem.

Specifically, each iteration of Algorithm 1 need to solve a quadratic programming (QP) problem. In general, the time complexity of solving such a QP problem is $O((2n)^3)$, where n denotes the number of training samples. However, by employing the clipDCD algorithm (Boyd, 2004), we can reduce the complexity of each coordinate update to $O(2n)$. The clipDCD algorithm’s overall time complexity is $O(t(2n))$ if convergence occurs after t iterations. Therefore, we adopt the clipDCD algorithm for the BAEN-SVM subproblem. Let q denote the number of iterations required for convergence for the half-quadratic optimization procedure. Then, the overall time complexity for computing Algorithm 1 is $O(qt(2n))$, where q and t refer to the number of HQ and clipDCD iterations, respectively. Consequently, compared to the direct solution method with complexity $O(q(2n)^3)$, implementing the clipDCD-based HQ optimization method significantly reduces computational complexity, especially for large-scale datasets.

5. Experiments

5.1. Set up

In this section, we present several experiments to evaluate the performance of the proposed BAEN-SVM on both artificial and benchmark datasets. For fair assessment and comprehensive comparison, the comparison models include well-known or recently proposed SVMs, such as Hinge-SVM (Cortes and Vapnik, 1995), Pin-SVM (Huang et al., 2014b), ALS-SVM (Huang et al., 2014a), EN-SVM (Qi et al., 2019), BQ-SVM (Zhang and Yang, 2024), BALS-SVM (Zhang and Yang, 2025). The algorithms are conducted in R 4.4.2, and the experiments are operated on the machine equipped with the AMD Ryzen 7 8845H CPU (3.80 GHz) and 32GB of RAM.

Five-fold cross-validation and grid search methods are applied to select the optimal settings for each model. The parameters p in ALS-SVM, BALS-SVM and BAEN-SVM are selected from $\{0.5, 0.7, 0.9, 0.99, 0.999\}$

, $\{0.3, 0.5, 0.7, 0.9, 0.99\}$ and $\{0.3, 0.5, 0.7\}$, respectively. The parameters τ in BAEN-SVM, BQ-SVM and Pin-SVM are selected from $\{0, 0.1, 0.3, 0.6, 1\}$, $\{0, 0.1, 0.3, 0.6, 1\}$ and $\{0.1, 0.3, 0.6, 1\}$, respectively. The parameters η of BALS-SVM, BQ-SVM, and BAEN-SVM takes on values in $\{2^{-6}, 2^{-4}, \dots, 2^4, 2^6\}$. The parameter C_1 and C_2 in EN-SVM have a range of values between $\{2^{-8}, 2^{-6}, 2^{-4}, \dots, 2^4, 2^6, 2^8\}$. For grid-searching the SVM regularization parameter C , we have $C \in \{2^i\}$, where $i \in \{-8, -7, \dots, 8\}$. For the nonlinear case, we use a radial basis function (RBF) kernel

$$K(x_i, x_j) = \exp(-\sigma \|x_i - x_j\|_2^2), \quad (79)$$

with σ chosen from $\{2^{-4}, 2^{-3}, \dots, 2^3, 2^4\}$.

The accuracy (ACC) and F_1 -score (F_1) are used to evaluate the classification performance of BAEN-SVM. Accuracy measures the proportion of samples correctly predicted by the model out of the total samples, which is defined as

$$ACC = \frac{TP + TN}{TP + TN + FP + FN}, \quad (80)$$

The F1 score is the reconciled average of precision and recall, which is expressed as

$$F_1 = \frac{2TP}{2TP + FP + FN}, \quad (81)$$

where TP and TN represent the number of correctly predicted positive and negative samples, respectively, while FP and FN reflect the number of misclassified positive and negative samples.

5.2. Artificial Datasets

We create a two-dimensional artificial dataset of 150 samples equally divided between two classes. Positive and negative samples are drawn from normal distributions with $\mu_+ = (3, 3)^T$ and $\mu_- = (-3, -3)^T$, respectively, and share the covariance matrix $V = \text{diag}(1, 1)$. For this experiment, the Bayes classifier is given by $f_C(x) = x_1 - x_2$.

Case 1. We introduce three outliers (label noise) into the negative class to simulate data contamination. Fig. 4 illustrates a comparison of the classification boundaries (black solid line) derived from six SVMs with the Bayes optimum boundary (green solid line). The deviation of each model's decision boundary from the Bayes classifier reflects its sensitivity to the introduced label noise.

In Fig. 4, BAEN-SVM exhibits the most stable performance in the presence of outliers, closely aligning with the Bayes optimal boundary and outperforming the other methods. LS-SVM and Pin-SVM follow, with their classification decisions slightly deviating from the Bayes classifier due to label noise. In contrast, Hinge-SVM and EN-SVM perform poorly, as their decision boundaries significantly deviate from the Bayes classifier, highlighting their high sensitivity to label noise.

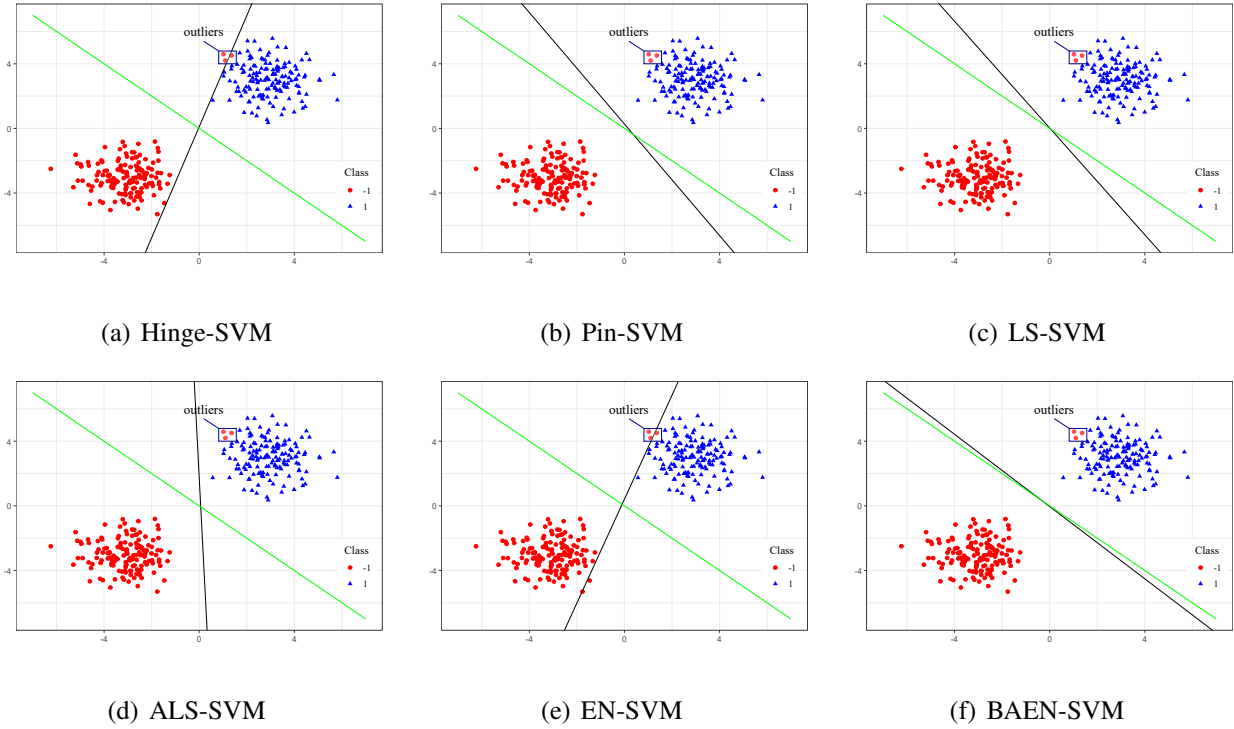


Fig. 4. Linear separating hyperplanes(black solid lines of Hing-SVM,Pin-SVM,LS-SVM,ALS-SVM,EN-SVM,BAEN-SVM. The green solid line is the Bayes classifier.

Case 2. In this case, three outliers are introduced into both the positive and negative classes. Fig. 5 displays the training samples along with the decision boundaries (black solid lines) generated by six different SVM models. The green solid line is the Bayes classifier.

As shown in Fig. 5, BAEN-SVM maintains superior classification performance even when outliers are added to both classes. In contrast, EN-SVM and Hinge-SVM are significantly affected by the outliers. Their decision boundaries deviate significantly and even intersect the outlier points, which indicates they appear to be overfitted. While Pin-SVM and LS-SVM exhibit some deviation from the Bayes optimal boundary, their performance still outperforms that of ALS-SVM, Hinge-SVM, and EN-SVM. Overall, BAEN-SVM exhibits the strongest robustness among all models, which aligns with its boundness. This result is consistent with the theoretical conclusion in Theorem 4, which further validates that BAEN-SVM is highly robust to label noise.

5.3. Benchmark Datasets

We select 15 datasets from the UCI machine learning repository¹ and the homepage of KEEL² to further validate the competitive performance of BAEN-SVM. Detailed descriptions of datasets are provided in Table 1. To further assess the robustness to noise, we artificially add 25% label noise by randomly swapping 25% labels

¹<https://archive.ics.uci.edu/>

²<https://sci2s.ugr.es/keel/datasets.php>

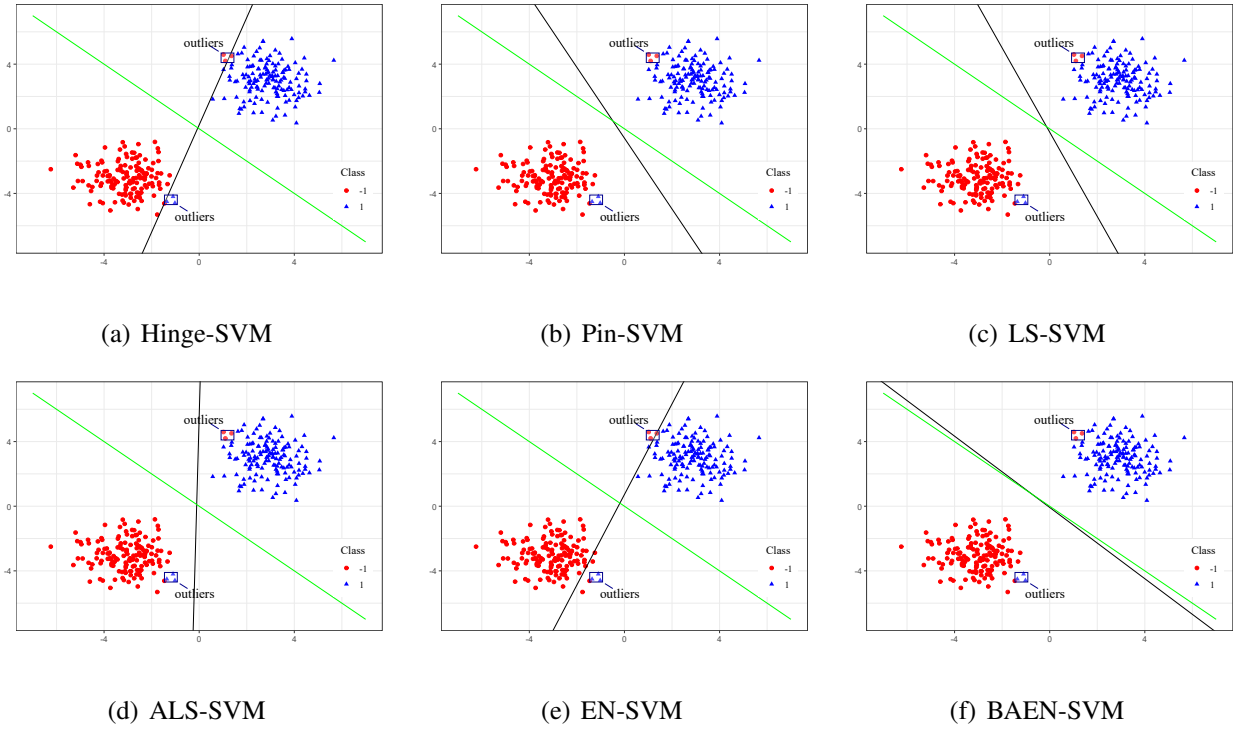


Fig. 5. Linear separating hyperplanes(black solid lines of Hing-SVM,Pin-SVM,LS-SVM,ALS-SVM,EN-SVM,BAEN-SVM. The green solid line is the Bayes classifier.

Table 1: Description of fifteen benchmark datasets

ID	Dataset	Samples	Attributes
1	appendicitis	106	7
2	australian	690	14
3	biodeg	1055	41
4	blood	748	4
5	bupa	345	6
6	darwin	174	450
7	diabetic	1151	19
8	fertility	100	9
9	haberman	306	3
10	pima	768	8
11	plrx	182	12
12	pop failures	540	20
13	raisin	900	7
14	saheart	462	9
15	sonar	208	60

in all samples. Additionally, feature noise is added by generating zero-mean Gaussian noise for each feature, with the noise variance scaled by the feature’s original variance. The noise level is controlled by the ratio r , which represents the proportion of the noise variance relative to the feature variance. The results of BAEN-SVM and the baseline models with linear kernel based on five-fold cross-validation are shown in [Table 2](#) and [Table 3](#). The results for Gaussian kernel are shown in [Table 4](#) and [Table 5](#).

From [Table 4](#) and [Table 5](#), our proposed BAEN-SVM with the Gaussian kernel outperforms other methods in most cases. In [Table 2](#) and [Table 3](#), BALS-SVM with the linear kernel shows competitiveness in comparison to BAEN-SVM. Moreover, for the case without noise and with 25% feature noise, EN-SVM performs better than Pin-SVM and ALS-SVM, highlighting the advantages of the elastic net hinge loss. However, when 25% label noise is added, EN-SVM’s performance drops due to the lack of robustness in the elastic net loss. Since the BAEN loss is designed to enjoy outlier insensitivity and resampling stability, it consistently achieves the highest average prediction accuracy and F_1 score under both label and feature noise.

5.4. Comparisons by statistical test

In this section, we apply the Friedman test ([Demšar, 2006](#)) to evaluate whether there are statistically significant differences between the seven SVM models across 15 datasets. The null hypothesis of the Friedman test assumes that all models perform equivalently. The test statistic F_F follows an F distribution with degrees of freedom ($F(k - 1, (k - 1)(N - 1))$), where $N = 15$ is the number of datasets and $k = 7$ is the number of classifiers. The F_F statistic is defined as

$$F_F = \frac{(N - 1)\chi_F^2}{N(k - 1) - \chi_F^2}. \quad (82)$$

where χ_F^2 is the raw Friedman statistic, given by

$$\chi_F^2 = \frac{12N}{k(k + 1)} \left(\sum_{j=1}^k R_j^2 - \frac{k(k + 1)^2}{4} \right), \quad (83)$$

where R_j is the average rank of the j -th classifier. The results for F_F and χ_F^2 for each type of kernel and noise are listed in [Table 6](#). At the level of significance of $\alpha = 0.05$, the critical value is $F_\alpha(6, 84) = 2.21$. Since all F_F values exceed this threshold, we conclude that there are statistically significant differences among the seven SVM models.

Next, we apply the Nemenyi post-hoc test to examine the specific distinctions among the classifiers. According to the Nemenyi test, two classifiers are considered significantly different if the difference in their average ranks exceeds the critical difference (CD). The CD is computed as

$$CD = q_{0.1}(k) \sqrt{\frac{k(k + 1)}{6N}} = 2.693 \times \sqrt{\frac{7 \times (7 + 1)}{6 \times 15}} = 2.12, \quad (84)$$

Table 2: Comparison of the mean accuracy (ACC±sd) of seven SVMs with linear kernel in benchmark datasets.

(a) 0% noise							
dataset	Hinge-SVM	Pin-SVM	ALS-SVM	EN-SVM	BQ-SVM	BALS-SVM	BAEN-SVM
appendicitis	0.886±0.064	0.887±0.055	0.886±0.072	0.905±0.075	0.895±0.078	0.895±0.078	0.895±0.078
australian	0.859±0.040	0.857±0.039	0.878±0.017	0.868±0.021	0.875±0.013	0.881±0.015	0.881±0.015
biodeg	0.872±0.019	0.867±0.017	0.868±0.014	0.871±0.009	0.877±0.024	0.869±0.021	0.873±0.020
blood	0.767±0.028	0.771±0.027	0.777±0.028	0.777±0.030	0.774±0.032	0.777±0.028	0.778±0.027
bupa	0.696±0.034	0.690±0.028	0.687±0.048	0.690±0.043	0.716±0.033	0.704±0.042	0.704±0.030
darwin	0.839±0.044	0.845±0.044	0.845±0.039	0.822±0.055	0.850±0.038	0.845±0.026	0.850±0.038
diabetic	0.714±0.017	0.706±0.019	0.729±0.018	0.735±0.030	0.739±0.024	0.729±0.021	0.732±0.016
fertility	0.880±0.027	0.880±0.027	0.870±0.027	0.880±0.027	0.880±0.027	0.880±0.027	0.890±0.042
haberman	0.741±0.083	0.745±0.071	0.751±0.072	0.755±0.055	0.752±0.061	0.751±0.070	0.751±0.047
pima	0.764±0.051	0.770±0.031	0.763±0.044	0.773±0.046	0.775±0.040	0.775±0.035	0.780±0.030
plrx	0.714±0.126	0.714±0.126	0.714±0.126	0.714±0.126	0.720±0.124	0.720±0.124	0.726±0.130
pop failures	0.957±0.014	0.944±0.020	0.965±0.010	0.965±0.010	0.961±0.018	0.965±0.012	0.952±0.021
raisin	0.872±0.010	0.873±0.014	0.869±0.008	0.870±0.010	0.877±0.013	0.877±0.016	0.880±0.011
saheart	0.745±0.071	0.741±0.071	0.745±0.052	0.745±0.060	0.741±0.069	0.751±0.066	0.751±0.066
sonar	0.770±0.102	0.765±0.114	0.774±0.086	0.779±0.060	0.794±0.056	0.785±0.091	0.789±0.073
(b) 25% label noise							
dataset	Hinge-SVM	Pin-SVM	ALS-SVM	EN-SVM	BQ-SVM	BALS-SVM	BAEN-SVM
appendicitis	0.895±0.078	0.887±0.043	0.877±0.055	0.895±0.071	0.914±0.062	0.905±0.075	0.905±0.075
australian	0.858±0.036	0.862±0.036	0.864±0.019	0.857±0.027	0.875±0.017	0.871±0.012	0.875±0.015
biodeg	0.825±0.033	0.823±0.030	0.834±0.022	0.832±0.028	0.834±0.041	0.837±0.023	0.834±0.023
blood	0.773±0.030	0.773±0.030	0.775±0.034	0.775±0.034	0.774±0.028	0.778±0.039	0.777±0.029
bupa	0.646±0.094	0.684±0.091	0.652±0.014	0.655±0.024	0.667±0.056	0.661±0.058	0.687±0.043
darwin	0.782±0.096	0.782±0.092	0.788±0.065	0.736±0.081	0.816±0.032	0.828±0.035	0.828±0.045
diabetic	0.634±0.031	0.644±0.042	0.661±0.034	0.665±0.027	0.674±0.021	0.675±0.010	0.684±0.022
fertility	0.820±0.130	0.810±0.102	0.810±0.102	0.830±0.125	0.890±0.042	0.880±0.045	0.890±0.042
haberman	0.745±0.073	0.745±0.073	0.755±0.061	0.755±0.061	0.751±0.075	0.761±0.065	0.755±0.072
pima	0.773±0.026	0.775±0.031	0.767±0.026	0.775±0.024	0.777±0.035	0.776±0.029	0.779±0.027
plrx	0.714±0.126	0.714±0.126	0.687±0.118	0.720±0.142	0.720±0.135	0.725±0.133	0.724±0.150
pop failures	0.915±0.022	0.915±0.022	0.909±0.029	0.919±0.025	0.922±0.011	0.919±0.023	0.919±0.023
raisin	0.871±0.009	0.867±0.014	0.866±0.009	0.872±0.014	0.873±0.011	0.870±0.013	0.873±0.021
saheart	0.728±0.068	0.725±0.059	0.714±0.050	0.721±0.058	0.732±0.071	0.732±0.070	0.732±0.071
sonar	0.755±0.095	0.755±0.067	0.764±0.059	0.760±0.044	0.765±0.069	0.765±0.086	0.765±0.064
(c) 25% feature noise							
dataset	Hinge-SVM	Pin-SVM	ALS-SVM	EN-SVM	BQ-SVM	BALS-SVM	BAEN-SVM
appendicitis	0.895±0.062	0.896±0.040	0.886±0.064	0.886±0.043	0.896±0.053	0.895±0.062	0.905±0.058
australian	0.870±0.014	0.867±0.043	0.878±0.016	0.878±0.022	0.874±0.014	0.880±0.025	0.875±0.024
biodeg	0.852±0.012	0.845±0.013	0.853±0.009	0.853±0.014	0.863±0.017	0.856±0.014	0.851±0.005
blood	0.767±0.024	0.767±0.024	0.777±0.027	0.779±0.039	0.771±0.030	0.777±0.027	0.775±0.028
bupa	0.658±0.022	0.652±0.043	0.661±0.024	0.670±0.038	0.681±0.042	0.681±0.025	0.684±0.039
darwin	0.828±0.020	0.833±0.024	0.850±0.025	0.828±0.020	0.856±0.022	0.850±0.025	0.856±0.036
diabetic	0.654±0.043	0.648±0.047	0.653±0.044	0.655±0.053	0.652±0.055	0.657±0.033	0.659±0.045
fertility	0.880±0.027	0.880±0.027	0.880±0.027	0.880±0.027	0.890±0.022	0.880±0.027	0.890±0.042
haberman	0.738±0.079	0.738±0.074	0.745±0.084	0.748±0.073	0.751±0.079	0.768±0.063	0.751±0.063
pima	0.768±0.045	0.770±0.047	0.767±0.041	0.768±0.037	0.775±0.032	0.768±0.042	0.772±0.046
plrx	0.714±0.126	0.714±0.126	0.720±0.132	0.720±0.132	0.725±0.140	0.736±0.059	0.726±0.124
pop failures	0.939±0.014	0.926±0.017	0.941±0.030	0.950±0.011	0.946±0.012	0.937±0.012	0.946±0.022
raisin	0.868±0.012	0.873±0.008	0.873±0.007	0.872±0.009	0.872±0.009	0.874±0.012	0.874±0.012
saheart	0.740±0.058	0.738±0.060	0.747±0.057	0.743±0.070	0.741±0.065	0.743±0.069	0.747±0.071
sonar	0.755±0.074	0.760±0.081	0.760±0.102	0.760±0.043	0.775±0.094	0.779±0.113	0.789±0.101

Table 3: Comparison of the mean F_1 -score ($F_1 \pm sd$) of seven SVMs with linear kernel in benchmark datasets.

(a) 0% noise							
dataset	Hinge-SVM	Pin-SVM	ALS-SVM	EN-SVM	BQ-SVM	BALS-SVM	BAEN-SVM
appendicitis	0.931±0.038	0.933±0.033	0.930±0.043	0.943±0.045	0.936±0.046	0.936±0.046	0.936±0.046
australian	0.864±0.039	0.861±0.038	0.888±0.020	0.878±0.021	0.888±0.014	0.891±0.015	0.891±0.015
biodeg	0.904±0.015	0.901±0.014	0.900±0.013	0.903±0.009	0.908±0.018	0.902±0.016	0.905±0.017
blood	0.867±0.017	0.867±0.017	0.871±0.018	0.871±0.019	0.869±0.019	0.871±0.018	0.871±0.018
bupa	0.601±0.061	0.585±0.041	0.594±0.072	0.593±0.070	0.617±0.060	0.609±0.062	0.618±0.052
darwin	0.834±0.055	0.843±0.047	0.842±0.048	0.820±0.059	0.849±0.030	0.847±0.061	0.852±0.034
diabetic	0.736±0.022	0.735±0.025	0.744±0.028	0.744±0.019	0.751±0.030	0.750±0.034	0.748±0.029
fertility	0.936±0.016	0.936±0.016	0.930±0.016	0.936±0.016	0.936±0.016	0.936±0.016	0.941±0.023
haberman	0.846±0.054	0.849±0.055	0.848±0.054	0.849±0.056	0.849±0.055	0.850±0.046	0.852±0.038
pima	0.830±0.038	0.835±0.025	0.829±0.030	0.838±0.036	0.838±0.039	0.836±0.029	0.842±0.021
plrx	0.828±0.088	0.828±0.088	0.828±0.088	0.828±0.088	0.831±0.092	0.831±0.092	0.834±0.090
pop failures	0.698±0.141	0.572±0.084	0.743±0.115	0.748±0.047	0.753±0.123	0.750±0.122	0.610±0.138
raisin	0.868±0.022	0.869±0.017	0.864±0.010	0.866±0.008	0.874±0.010	0.872±0.014	0.877±0.014
saheart	0.811±0.061	0.816±0.052	0.815±0.045	0.815±0.050	0.814±0.052	0.821±0.047	0.823±0.050
sonar	0.786±0.039	0.771±0.062	0.791±0.055	0.800±0.054	0.809±0.058	0.803±0.077	0.791±0.094
(b) 25% label noise							
dataset	Hinge-SVM	Pin-SVM	ALS-SVM	EN-SVM	BQ-SVM	BALS-SVM	BAEN-SVM
appendicitis	0.936±0.046	0.932±0.026	0.923±0.059	0.935±0.042	0.947±0.038	0.942±0.045	0.942±0.045
australian	0.865±0.037	0.868±0.037	0.874±0.021	0.866±0.029	0.888±0.015	0.885±0.016	0.887±0.011
biodeg	0.868±0.028	0.867±0.023	0.875±0.019	0.874±0.023	0.875±0.034	0.877±0.020	0.876±0.016
blood	0.869±0.019	0.869±0.019	0.869±0.024	0.869±0.022	0.869±0.019	0.871±0.024	0.870±0.018
bupa	0.577±0.104	0.594±0.085	0.589±0.035	0.573±0.081	0.608±0.097	0.584±0.053	0.613±0.077
darwin	0.785±0.084	0.786±0.082	0.792±0.052	0.745±0.064	0.823±0.018	0.834±0.021	0.834±0.035
diabetic	0.636±0.045	0.663±0.044	0.653±0.033	0.660±0.027	0.719±0.010	0.720±0.019	0.721±0.011
fertility	0.895±0.085	0.888±0.098	0.884±0.072	0.902±0.075	0.941±0.023	0.936±0.016	0.941±0.023
haberman	0.845±0.052	0.846±0.052	0.848±0.050	0.848±0.043	0.850±0.054	0.851±0.048	0.850±0.052
pima	0.835±0.024	0.837±0.027	0.830±0.023	0.838±0.025	0.841±0.028	0.839±0.025	0.840±0.024
plrx	0.828±0.088	0.828±0.088	0.801±0.087	0.830±0.095	0.831±0.092	0.834±0.091	0.833±0.100
pop failures	0.208±0.102	0.234±0.147	0.216±0.063	0.229±0.057	0.367±0.145	0.262±0.028	0.297±0.106
raisin	0.865±0.007	0.862±0.009	0.863±0.008	0.867±0.006	0.868±0.008	0.865±0.017	0.869±0.011
saheart	0.802±0.055	0.805±0.046	0.792±0.034	0.805±0.046	0.809±0.040	0.809±0.039	0.810±0.036
sonar	0.745±0.129	0.753±0.092	0.764±0.082	0.760±0.063	0.762±0.067	0.765±0.099	0.767±0.052
(c) 25% feature noise							
dataset	Hinge-SVM	Pin-SVM	ALS-SVM	EN-SVM	BQ-SVM	BALS-SVM	BAEN-SVM
appendicitis	0.935±0.038	0.938±0.026	0.930±0.043	0.932±0.042	0.936±0.033	0.935±0.038	0.940±0.036
australian	0.880±0.017	0.874±0.026	0.888±0.016	0.887±0.023	0.886±0.012	0.889±0.026	0.887±0.012
biodeg	0.891±0.012	0.887±0.011	0.891±0.008	0.892±0.011	0.897±0.012	0.895±0.012	0.891±0.015
blood	0.867±0.016	0.867±0.016	0.871±0.018	0.870±0.017	0.867±0.018	0.871±0.018	0.870±0.018
bupa	0.504±0.080	0.553±0.116	0.558±0.185	0.560±0.127	0.605±0.112	0.599±0.060	0.589±0.074
darwin	0.826±0.038	0.833±0.036	0.849±0.041	0.823±0.041	0.854±0.036	0.849±0.041	0.854±0.050
diabetic	0.660±0.048	0.659±0.077	0.635±0.052	0.665±0.059	0.678±0.035	0.687±0.040	0.690±0.015
fertility	0.936±0.016	0.936±0.016	0.936±0.016	0.936±0.016	0.941±0.012	0.936±0.016	0.941±0.023
haberman	0.847±0.052	0.846±0.059	0.845±0.058	0.848±0.048	0.849±0.056	0.853±0.053	0.849±0.051
pima	0.833±0.036	0.836±0.036	0.835±0.031	0.834±0.029	0.839±0.031	0.835±0.035	0.839±0.035
plrx	0.828±0.088	0.828±0.088	0.831±0.091	0.831±0.091	0.834±0.094	0.831±0.091	0.834±0.086
pop failures	0.451±0.089	0.425±0.126	0.495±0.162	0.644±0.145	0.541±0.083	0.507±0.163	0.542±0.113
raisin	0.864±0.007	0.866±0.010	0.868±0.008	0.867±0.008	0.866±0.011	0.868±0.010	0.868±0.010
saheart	0.814±0.049	0.814±0.050	0.822±0.045	0.814±0.031	0.818±0.051	0.818±0.040	0.822±0.048
sonar	0.763±0.053	0.765±0.093	0.777±0.066	0.778±0.043	0.792±0.019	0.789±0.111	0.801±0.044

Table 4: Comparison of the mean accuracy (ACC±sd) of seven SVMs with RBF kernel in benchmark datasets.

(a) 0% noise							
dataset	Hinge-SVM	Pin-SVM	ALS-SVM	EN-SVM	BQ-SVM	BALS-SVM	BAEN-SVM
appendicitis	0.877±0.073	0.877±0.073	0.886±0.087	0.886±0.087	0.905±0.075	0.895±0.071	0.905±0.075
australian	0.871±0.014	0.871±0.024	0.872±0.022	0.871±0.018	0.872±0.026	0.872±0.022	0.872±0.022
biodeg	0.898±0.005	0.895±0.015	0.900±0.010	0.904±0.006	0.897±0.004	0.901±0.010	0.902±0.011
blood	0.793±0.043	0.794±0.042	0.797±0.050	0.799±0.045	0.795±0.043	0.798±0.040	0.799±0.034
bupa	0.704±0.047	0.710±0.043	0.713±0.040	0.713±0.040	0.736±0.043	0.725±0.065	0.722±0.055
darwin	0.753±0.050	0.753±0.050	0.753±0.050	0.753±0.050	0.753±0.050	0.753±0.050	0.775±0.054
diabetic	0.723±0.019	0.732±0.028	0.730±0.020	0.735±0.024	0.728±0.028	0.730±0.026	0.729±0.022
fertility	0.880±0.027	0.880±0.027	0.890±0.022	0.890±0.022	0.880±0.027	0.890±0.022	0.900±0.035
haberman	0.765±0.067	0.755±0.063	0.761±0.076	0.758±0.073	0.764±0.089	0.765±0.069	0.768±0.051
pima	0.768±0.044	0.767±0.045	0.768±0.051	0.770±0.042	0.772±0.040	0.769±0.051	0.772±0.039
plrx	0.725±0.133						
pop failures	0.948±0.017	0.944±0.020	0.944±0.020	0.948±0.017	0.948±0.017	0.944±0.020	0.950±0.011
raisin	0.871±0.016	0.874±0.008	0.873±0.010	0.876±0.010	0.877±0.007	0.876±0.016	0.877±0.009
saheart	0.727±0.047	0.734±0.036	0.740±0.051	0.743±0.053	0.743±0.045	0.743±0.057	0.745±0.043
sonar	0.909±0.045	0.909±0.045	0.909±0.045	0.914±0.046	0.909±0.045	0.909±0.045	0.914±0.036
(b) 25% label noise							
dataset	Hinge-SVM	Pin-SVM	ALS-SVM	EN-SVM	BQ-SVM	BALS-SVM	BAEN-SVM
appendicitis	0.895±0.078	0.895±0.085	0.895±0.078	0.895±0.078	0.905±0.075	0.905±0.075	0.914±0.062
australian	0.867±0.025	0.865±0.026	0.861±0.028	0.867±0.025	0.870±0.029	0.865±0.022	0.867±0.024
biodeg	0.839±0.018	0.838±0.021	0.841±0.024	0.842±0.023	0.842±0.017	0.844±0.026	0.844±0.029
blood	0.781±0.042	0.782±0.043	0.783±0.042	0.785±0.043	0.791±0.040	0.790±0.017	0.793±0.042
bupa	0.652±0.078	0.646±0.084	0.664±0.084	0.667±0.070	0.716±0.078	0.658±0.093	0.690±0.070
darwin	0.638±0.103	0.638±0.103	0.638±0.103	0.638±0.103	0.644±0.099	0.638±0.114	0.690±0.110
diabetic	0.659±0.034	0.662±0.037	0.663±0.024	0.663±0.024	0.661±0.031	0.665±0.028	0.666±0.033
fertility	0.880±0.027	0.880±0.027	0.880±0.027	0.880±0.027	0.890±0.042	0.880±0.027	0.890±0.114
haberman	0.761±0.063	0.761±0.061	0.758±0.068	0.761±0.073	0.768±0.058	0.764±0.067	0.771±0.043
pima	0.763±0.049	0.762±0.052	0.766±0.040	0.767±0.046	0.767±0.038	0.767±0.040	0.768±0.049
plrx	0.725±0.133						
pop failures	0.915±0.022	0.915±0.022	0.919±0.028	0.919±0.028	0.915±0.022	0.919±0.028	0.920±0.024
raisin	0.869±0.009	0.867±0.009	0.870±0.012	0.871±0.008	0.869±0.006	0.871±0.008	0.874±0.008
saheart	0.719±0.033	0.721±0.037	0.723±0.041	0.723±0.054	0.738±0.044	0.736±0.047	0.743±0.064
sonar	0.807±0.094	0.807±0.094	0.802±0.116	0.826±0.095	0.812±0.100	0.822±0.089	0.826±0.095
(c) 25% feature noise							
dataset	Hinge-SVM	Pin-SVM	ALS-SVM	EN-SVM	BQ-SVM	BALS-SVM	BAEN-SVM
appendicitis	0.877±0.073	0.877±0.073	0.886±0.087	0.886±0.087	0.886±0.064	0.886±0.064	0.895±0.078
australian	0.868±0.009	0.871±0.017	0.870±0.014	0.871±0.012	0.870±0.014	0.872±0.013	0.872±0.018
biodeg	0.882±0.019	0.883±0.021	0.882±0.018	0.884±0.019	0.883±0.022	0.883±0.024	0.884±0.024
blood	0.773±0.043	0.781±0.055	0.779±0.041	0.783±0.057	0.785±0.043	0.785±0.057	0.783±0.019
bupa	0.704±0.035	0.699±0.044	0.701±0.030	0.713±0.047	0.704±0.039	0.701±0.024	0.707±0.053
darwin	0.730±0.039	0.730±0.039	0.730±0.039	0.730±0.039	0.730±0.039	0.730±0.039	0.741±0.037
diabetic	0.665±0.036	0.665±0.042	0.672±0.036	0.676±0.036	0.671±0.031	0.673±0.032	0.674±0.032
fertility	0.890±0.022	0.900±0.035	0.900±0.035	0.890±0.022	0.900±0.035	0.900±0.035	0.910±0.042
haberman	0.742±0.072	0.748±0.073	0.758±0.084	0.758±0.084	0.758±0.064	0.758±0.068	0.761±0.075
pima	0.767±0.042	0.767±0.042	0.771±0.043	0.771±0.043	0.768±0.039	0.771±0.043	0.769±0.041
plrx	0.725±0.133						
pop failures	0.928±0.029	0.928±0.029	0.928±0.028	0.933±0.032	0.930±0.031	0.930±0.029	0.935±0.032
raisin	0.866±0.025	0.867±0.022	0.870±0.014	0.871±0.013	0.876±0.007	0.871±0.013	0.872±0.008
saheart	0.730±0.054	0.736±0.066	0.734±0.065	0.749±0.044	0.745±0.062	0.736±0.048	0.740±0.049
sonar	0.842±0.074	0.842±0.074	0.842±0.074	0.866±0.080	0.842±0.074	0.842±0.074	0.870±0.062

Table 5: Comparison of the mean F_1 -score ($F_1 \pm sd$) of seven SVMs with RBF kernel in benchmark datasets.

(a) 0% noise							
dataset	Hinge-SVM	Pin-SVM	ALS-SVM	EN-SVM	BQ-SVM	BALS-SVM	BAEN-SVM
appendicitis	0.926±0.043	0.926±0.043	0.931±0.051	0.931±0.051	0.942±0.045	0.937±0.046	0.942±0.045
australian	0.884±0.012	0.882±0.022	0.886±0.016	0.885±0.013	0.884±0.012	0.885±0.016	0.886±0.011
biodeg	0.923±0.007	0.920±0.014	0.925±0.010	0.928±0.006	0.922±0.006	0.926±0.010	0.926±0.010
blood	0.872±0.029	0.873±0.028	0.876±0.033	0.876±0.030	0.874±0.033	0.876±0.027	0.878±0.021
bupa	0.623±0.074	0.618±0.099	0.631±0.127	0.637±0.095	0.652±0.072	0.633±0.070	0.641±0.065
darwin	0.796±0.037	0.796±0.037	0.796±0.037	0.796±0.037	0.796±0.037	0.796±0.037	0.808±0.043
diabetic	0.733±0.021	0.742±0.029	0.727±0.035	0.729±0.022	0.741±0.020	0.731±0.033	0.739±0.018
fertility	0.936±0.016	0.936±0.016	0.941±0.012	0.941±0.012	0.936±0.016	0.941±0.012	0.946±0.019
haberman	0.852±0.046	0.847±0.042	0.851±0.052	0.849±0.052	0.856±0.052	0.855±0.047	0.857±0.033
pima	0.836±0.032	0.836±0.036	0.835±0.037	0.837±0.037	0.837±0.027	0.837±0.034	0.841±0.041
plrx	0.834±0.091						
pop failures	0.575±0.179	0.523±0.220	0.533±0.150	0.591±0.153	0.575±0.179	0.533±0.150	0.637±0.144
raisin	0.868±0.012	0.869±0.015	0.869±0.009	0.871±0.011	0.873±0.009	0.871±0.011	0.873±0.011
saheart	0.815±0.036	0.815±0.036	0.817±0.038	0.817±0.047	0.823±0.028	0.819±0.041	0.821±0.034
sonar	0.915±0.045	0.915±0.045	0.915±0.045	0.919±0.046	0.915±0.045	0.915±0.045	0.922±0.032
(b) 25% label noise							
dataset	Hinge-SVM	Pin-SVM	ALS-SVM	EN-SVM	BQ-SVM	BALS-SVM	BAEN-SVM
appendicitis	0.936±0.046	0.935±0.053	0.936±0.046	0.936±0.046	0.942±0.045	0.942±0.045	0.947±0.038
australian	0.882±0.021	0.881±0.020	0.881±0.023	0.881±0.020	0.881±0.019	0.880±0.024	0.882±0.024
biodeg	0.878±0.015	0.877±0.018	0.879±0.019	0.879±0.019	0.880±0.014	0.880±0.021	0.881±0.021
blood	0.870±0.026	0.870±0.027	0.871±0.026	0.872±0.026	0.874±0.030	0.872±0.033	0.876±0.031
bupa	0.595±0.103	0.592±0.086	0.596±0.162	0.606±0.105	0.630±0.138	0.614±0.117	0.640±0.083
darwin	0.683±0.092	0.683±0.092	0.683±0.092	0.683±0.092	0.686±0.091	0.687±0.101	0.714±0.097
diabetic	0.662±0.029	0.664±0.041	0.662±0.030	0.663±0.031	0.685±0.021	0.681±0.024	0.686±0.026
fertility	0.936±0.016	0.936±0.016	0.936±0.016	0.936±0.016	0.941±0.023	0.936±0.016	0.941±0.023
haberman	0.851±0.043	0.851±0.043	0.849±0.046	0.853±0.056	0.854±0.048	0.854±0.050	0.857±0.033
pima	0.834±0.036	0.833±0.039	0.832±0.038	0.835±0.034	0.838±0.031	0.835±0.038	0.836±0.036
plrx	0.834±0.091						
pop failures	0.217±0.072	0.224±0.075	0.247±0.073	0.277±0.077	0.326±0.178	0.296±0.155	0.313±0.119
raisin	0.862±0.010	0.859±0.010	0.865±0.014	0.865±0.014	0.863±0.010	0.866±0.014	0.870±0.013
saheart	0.815±0.030	0.815±0.030	0.820±0.029	0.818±0.030	0.822±0.034	0.820±0.029	0.822±0.040
sonar	0.817±0.098	0.817±0.098	0.810±0.118	0.835±0.111	0.823±0.100	0.834±0.089	0.838±0.093
(c) 25% feature noise							
dataset	Hinge-SVM	Pin-SVM	ALS-SVM	EN-SVM	BQ-SVM	BALS-SVM	BAEN-SVM
appendicitis	0.926±0.043	0.926±0.043	0.931±0.051	0.931±0.051	0.931±0.051	0.931±0.051	0.936±0.046
australian	0.882±0.011	0.884±0.016	0.885±0.010	0.885±0.010	0.883±0.014	0.886±0.008	0.885±0.008
biodeg	0.910±0.016	0.911±0.016	0.910±0.014	0.912±0.014	0.911±0.017	0.913±0.019	0.913±0.017
blood	0.868±0.016	0.868±0.032	0.868±0.033	0.869±0.027	0.873±0.022	0.872±0.032	0.873±0.011
bupa	0.603±0.079	0.597±0.074	0.598±0.058	0.622±0.082	0.606±0.088	0.609±0.074	0.613±0.089
darwin	0.781±0.031	0.781±0.031	0.781±0.031	0.781±0.031	0.781±0.031	0.781±0.031	0.789±0.036
diabetic	0.680±0.041	0.682±0.045	0.682±0.034	0.687±0.043	0.688±0.045	0.687±0.022	0.697±0.027
fertility	0.941±0.012	0.946±0.019	0.946±0.019	0.941±0.012	0.946±0.019	0.946±0.019	0.952±0.022
haberman	0.846±0.050	0.847±0.055	0.852±0.050	0.855±0.061	0.852±0.055	0.852±0.050	0.855±0.051
pima	0.833±0.034	0.834±0.034	0.837±0.036	0.835±0.035	0.836±0.044	0.837±0.036	0.839±0.031
plrx	0.834±0.091						
pop failures	0.268±0.281	0.319±0.252	0.319±0.252	0.372±0.268	0.319±0.252	0.326±0.261	0.463±0.169
raisin	0.857±0.030	0.858±0.027	0.863±0.016	0.864±0.016	0.871±0.007	0.866±0.016	0.866±0.016
saheart	0.818±0.031	0.818±0.031	0.820±0.030	0.821±0.036	0.823±0.041	0.819±0.034	0.821±0.021
sonar	0.854±0.071	0.854±0.071	0.854±0.071	0.877±0.042	0.854±0.071	0.854±0.071	0.880±0.061

Table 6: The result of Friedman test on seven classifiers.

Table	Kernel	evaluation index	Noise	χ_F^2	F_F
Table 2	linear	ACC	without noise	41.76	12.11
			25% label noise	59.23	26.95
			25% feature noise	31.46	7.53
Table 3	linear	F_1	without noise	39.50	10.95
			25% label noise	47.88	15.91
			25% feature noise	30.54	7.19
Table 4	Gaussianl	ACC	without noise	19.83	3.96
			25% label noise	37.72	10.1
			25% feature noise	16.33	3.1
Table 5	Gaussian	F_1	without noise	21.06	4.28
			25% label noise	26.49	5.84
			25% feature noise	24.35	5.19

where $q_{0.1} = 2.693$. We used *CD* diagrams Fig. 6 and Fig. 7 to compare the average rankings of each SVM with different kernels and noise types. The top line shows the average ranks, with colors changing from blue to black. Groups of algorithms with no significant differences are linked with a red line.

As shown in Fig. 6, BAEN-SVM outperforms all other SVM models in terms of ACC evaluation criterion, and its advantage becomes apparent when there is 25% label noise and feature noise. In Fig. 6(b) and Fig. 7(e), BAEN-SVM markedly differs from EN-SVM, demonstrating that BAEN-SVM addresses the limitation of EN-SVM in label noise. When faced with 25% feature noise in Fig. 6(c) and Fig. 6(f), BAEN-SVM, BALS-SVM, BQ-SVM, and EN-SVM show similar performance levels, all significantly outperforming ALS-SVM, Hinge-SVM, and Pin-SVM. In Fig. 6(a)-(f), BAEN-SVM’s average rank with the RBF kernel is notably higher than with the linear kernel. BAEN-SVM consistently surpasses other models, particularly Hinge-SVM and Pin-SVM, which continue to perform poorly. Fig. 7 illustrates that the average rank of the models based on the F_1 evaluation criterion is similar to that of the ACC.

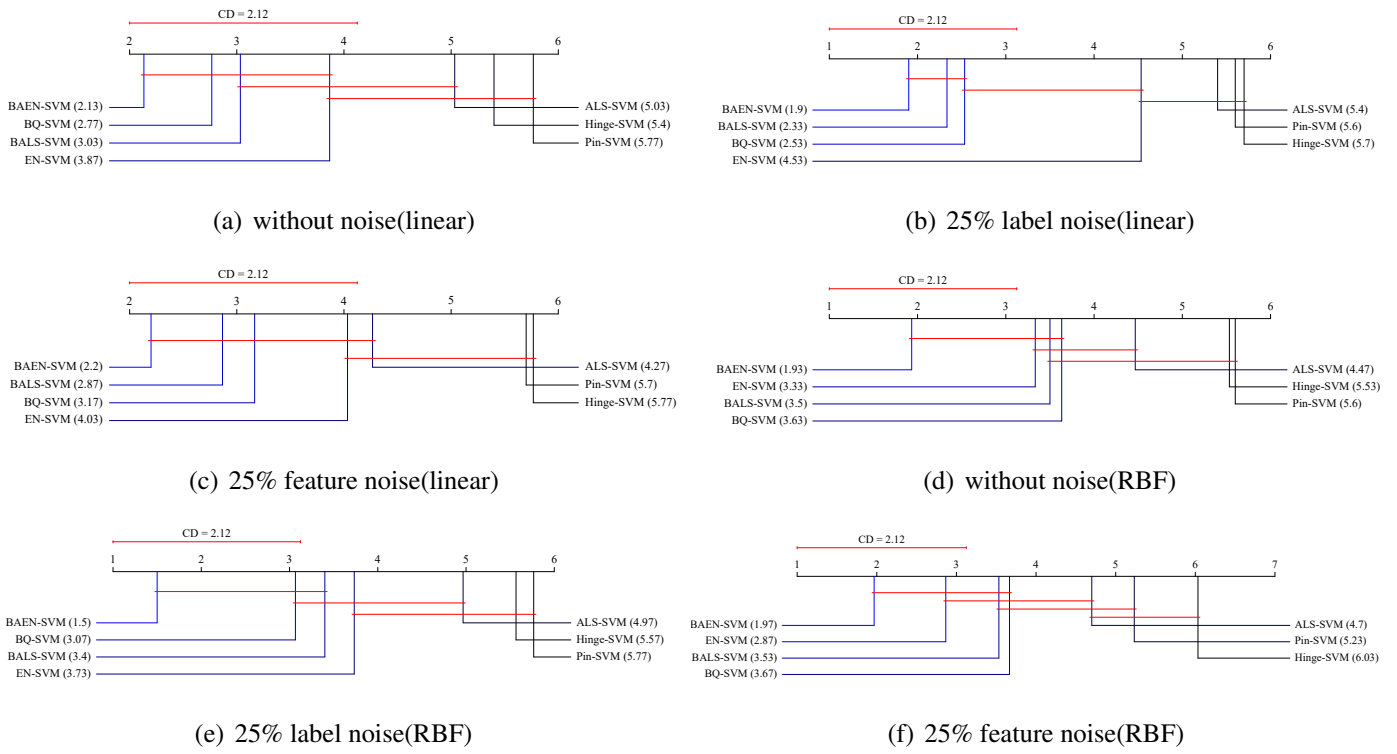


Fig. 6. Comparison ACC with the Nemenyi test

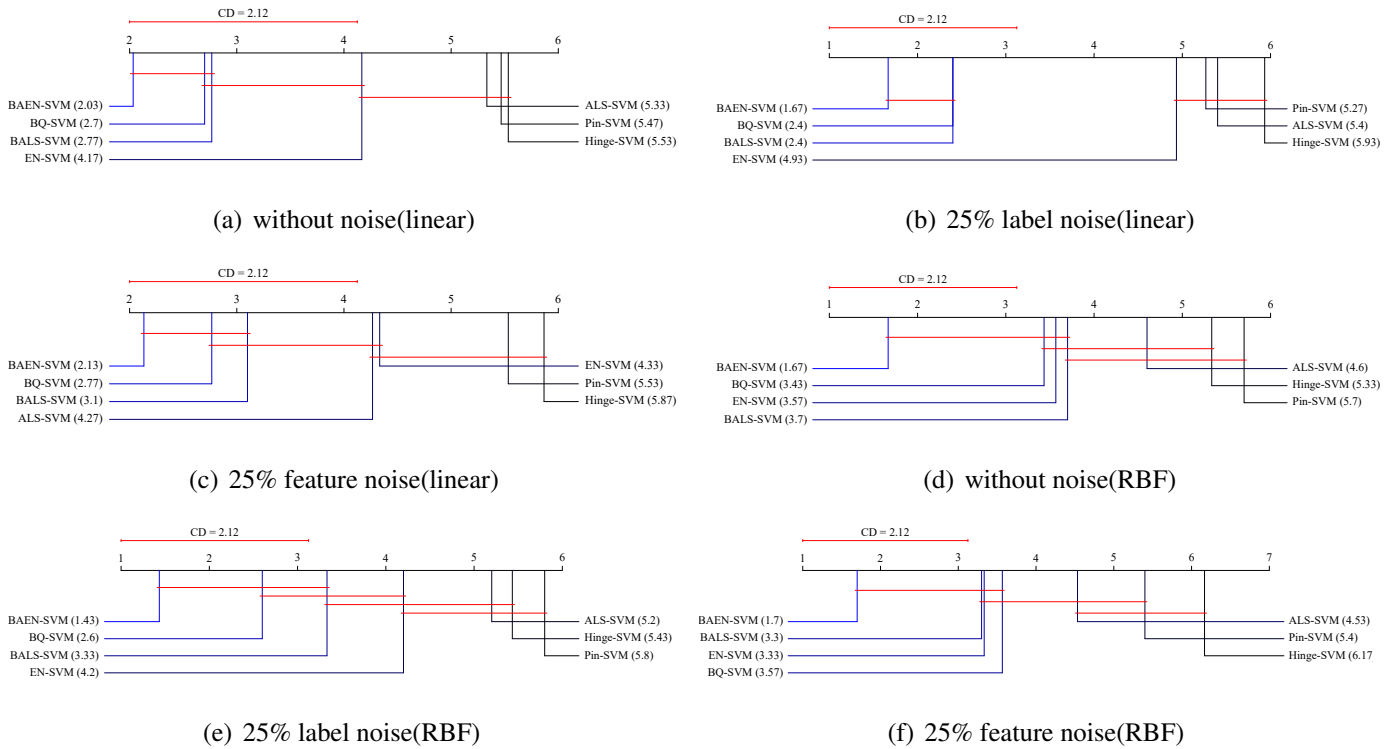


Fig. 7. Comparison F_1 with the Nemenyi test

6. Conclusion

In this paper, we propose BAEN-SVM by combining a new bounded asymmetric elastic net loss function L_{baen} with SVM. To solve the non-convex optimization, we introduce a clipDCD-based HQ algorithm to solve the model. Through an analysis of the HQ optimization, we show that BAEN-SVM can be viewed as an AEN-WSVM, thereby transforming the original non-convex problem into a convex surrogate, which is solved using the clipDCD algorithm. Further theoretical analysis demonstrates that BAEN-SVM possesses desirable properties, including Fisher consistency and noise insensitivity, ensuring its robustness and generalization ability in practical applications. Additionally, the VTUB provides further evidence of the favorable geometric properties of BAEN-SVM. Experimental results on both artificial and benchmark datasets confirm that BAEN-SVM outperforms other models, achieving superior performance on both clean and noise-contaminated datasets. Statistical tests further validate its advantages.

Despite these strengths, there are several important issues for future investigation: (i) While the clipDCD-based HQ optimization model performs stably on small-scale datasets, its computational efficiency is limited when applied to large-scale datasets due to the need to solve a quadratic programming problem at each iteration. Improving the efficiency of the optimization algorithm and expanding the scalability of BAEN-SVM for large-scale applications are key directions for future research. (ii) The violation tolerance upper bound of BAEN-SVM currently applies only to two constraint-violating samples within the same class. To extend this property to any two samples in the same class, a one-to-one correspondence between the slack variable ξ_i and the Lagrange multiplier α_i must be established, with the additional condition that $\alpha_i \neq 0$ when $\xi_i = 0$. These issues warrant further exploration in future work.

References

- Bhatia, R., 2013. Matrix analysis. volume 169. Springer Science & Business Media.
- Boyd, S., 2004. Convex optimization. Cambridge UP .
- Cortes, C., Vapnik, V., 1995. Support-vector networks. *Machine Learning* 20, 273–297.
- Demšar, J., 2006. Statistical comparisons of classifiers over multiple data sets. *Journal of Machine Learning Research* 7, 1–30.
- Fu, S., Tian, Y., Tang, L., 2023. Robust regression under the general framework of bounded loss functions. *European Journal of Operational Research* 310, 1325–1339.
- Fu, S., Wang, X., Tang, J., Lan, S., Tian, Y., 2024. Generalized robust loss functions for machine learning. *Neural Networks* 171, 200–214.

- Hampel, F.R., 1974. The influence curve and its role in robust estimation. *Journal of the American Statistical Association* 69, 383–393.
- Huang, X., Shi, L., Suykens, J.A.K., 2014a. Asymmetric least squares support vector machine classifiers. *Computational Statistics & Data Analysis* 70, 395–405.
- Huang, X., Shi, L., Suykens, J.A.K., 2014b. Support vector machine classifier with pinball loss. *IEEE Transactions on Pattern Analysis and Machine Intelligence* 36, 984–997.
- Kuo, R., Chiu, T.H., 2024. Hybrid of jellyfish and particle swarm optimization algorithm-based support vector machine for stock market trend prediction. *Applied Soft Computing* 154, 111394.
- Li, H.J., Qiu, Z.B., Wang, M.M., Zhang, C., Hong, H.Z., Fu, R., Peng, L.S., Huang, C., Cui, Q., Zhang, J.T., et al., 2025. Radiomics-based support vector machine distinguishes molecular events driving the progression of lung adenocarcinoma. *Journal of Thoracic Oncology* 20, 52–64.
- Ma, Y., Zhang, Q., Li, D., Tian, Y., 2019. Linex support vector machine for large-scale classification. *IEEE Access* 7, 70319–70331.
- Mangasarian, O.L., Musicant, D.R., 2001. Lagrangian support vector machines. *Journal of Machine Learning Research* 1, 161–177.
- Peng, X., Chen, D., Kong, L., 2014. A clipping dual coordinate descent algorithm for solving support vector machines. *Knowledge-Based Systems* 71, 266–278.
- Qi, K., Yang, H., 2022. Elastic net nonparallel hyperplane support vector machine and its geometrical rationality. *IEEE Transactions on Neural Networks and Learning Systems* 33, 7199–7209.
- Qi, K., Yang, H., 2023. Capped asymmetric elastic net support vector machine for robust binary classification. *International Journal of Intelligent Systems* 2023, 2201330.
- Qi, K., Yang, H., Hu, Q., Yang, D., 2019. A new adaptive weighted imbalanced data classifier via improved support vector machines with high-dimension nature. *Knowledge-Based Systems* 185, 104933.
- Shen, X., Niu, L., Qi, Z., Tian, Y., 2017. Support vector machine classifier with truncated pinball loss. *Pattern Recognition* 68, 199–210.
- Tang, J., Li, J., Xu, W., Tian, Y., Ju, X., Zhang, J., 2021a. Robust cost-sensitive kernel method with blinex loss and its applications in credit risk evaluation. *Neural Networks* 143, 327–344.
- Tang, L., Tian, Y., Li, W., Pardalos, P.M., 2021b. Valley-loss regular simplex support vector machine for robust multiclass classification. *Knowledge-Based Systems* 216, 106801.
- Vapnik, V., 2006. Estimation of dependences based on empirical data. Springer Science & Business Media.
- Vapnik, V.N., 1999. An overview of statistical learning theory. *IEEE transactions on neural networks* 10,

988–999.

- Wang, H., Liu, Y., Zhang, S., 2023. Smooth and semi-smooth pinball twin support vector machine. *Expert Systems with Applications* 226, 120189.
- Wang, H., Shao, Y., 2023. Fast truncated huber loss svm for large scale classification. *Knowledge-Based Systems* 260, 110074.
- Wang, H., Shao, Y., 2024. Fast generalized ramp loss support vector machine for pattern classification. *Pattern Recognition* 146, 109987.
- Wang, L., Jia, H., Li, J., 2008. Training robust support vector machine with smooth ramp loss in the primal space. *Neurocomputing* 71, 3020–3025.
- Wang, X., 2025. Khatri-rao factorization based bi-level support vector machine for hyperspectral image classification. *IEEE Journal of Selected Topics in Applied Earth Observations and Remote Sensing* .
- Wang, X., Jiang, Y., Huang, M., Zhang, H., 2013. Robust variable selection with exponential squared loss. *Journal of the American Statistical Association* 108, 632–643.
- Wu, Y., Liu, Y., 2007. Robust truncated hinge loss support vector machines. *Journal of the American Statistical Association* 102, 974–983.
- Xu, G., Hu, B., Principe, J.C., 2018. Robust C-loss kernel classifiers. *IEEE Transactions on Neural Networks and Learning Systems* 29, 510–522.
- Zhang, J., Yang, H., 2024. Bounded quantile loss for robust support vector machines-based classification and regression. *Expert Systems with Applications* 242, 122759.
- Zhang, J., Yang, H., 2025. Robust support vector machine based on the bounded asymmetric least squares loss function and its applications in noise corrupted data. *Advanced Engineering Informatics* 65, 103371.
- Zhang, X.Y., Zhang, X.P., Yu, H.G., Liu, Q.S., 2025. A confident learning-based support vector machine for robust ground classification in noisy label environments. *Tunnelling and Underground Space Technology* 155, 106128.
- Zhu, W., Song, Y., Xiao, Y., 2020. Support vector machine classifier with huberized pinball loss. *Engineering Applications of Artificial Intelligence* 91, 103635.